

U.S. DEPARTMENT OF COMMERCE
National Technical Information Service

AD-A036 503

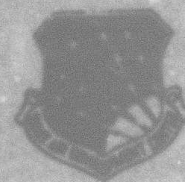
PROPAGATION OF MULTIWAVELENGTH LASER
RADIATION THROUGH ATMOSPHERIC TURBULENCE

OREGON GRADUATE CENTER
BEAVERTON

JANUARY 1977

ADA036503

RADC-TR-77-18
Final Technical Report
January 1977



PROPAGATION OF MULTIWAVELENGTH LASER RADIATION
THROUGH ATMOSPHERIC TURBULENCE

Oregon Graduate Center

Sponsored by
Defense Advanced Research Projects Agency (DoD)
ARPA Order No. 1279

Approved for public release;
distribution unlimited.



The views and conclusions contained in this document are those of the authors and should not be interpreted as necessarily representing the official policies, either expressed or implied, of the Defense Advanced Research Projects Agency or the U. S. Government.

REPRODUCED BY
NATIONAL TECHNICAL
INFORMATION SERVICE
U. S. DEPARTMENT OF COMMERCE
SPRINGFIELD, VA. 22161

HOME AIR DEVELOPMENT CENTER
AIR FORCE SYSTEMS COMMAND
GRIFFISS AIR FORCE BASE, NEW YORK 13441

BEST AVAILABLE COPY

SECURITY CLASSIFICATION OF THIS PAGE (When Data Entered)

REPORT DOCUMENTATION PAGE		READ INSTRUCTIONS BEFORE COMPLETING FORM
1. REPORT NUMBER RADC-TR-77-18	2. GOVT ACCESSION NO.	3. RECIPIENT'S CATALOG NUMBER
4. TITLE (and Subtitle) PROPAGATION OF MULTIWAVELENGTH LASER RADIATION THROUGH ATMOSPHERIC TURBULENCE		5. TYPE OF REPORT & PERIOD COVERED Final Technical Report 1 Feb 76 - 30 Nov 76
		6. PERFORMING ORG. REPORT NUMBER N/A
7. AUTHOR(s) J. Richard Kerr J. Fred Holmes Richard A. Elliott Myung H. Lee Michael E. Fossey Philip A Pincus		8. CONTRACT OR GRANT NUMBER(s) F30602-74-C-0082
9. PERFORMING ORGANIZATION NAME AND ADDRESS Oregon Graduate Center 19600 N. W. Walker Road Beaverton OR 97005		10. PROGRAM ELEMENT, PROJECT, TASK AREA & WORK UNIT NUMBERS 62301E 12790212
11. CONTROLLING OFFICE NAME AND ADDRESS Defense Advanced Research Projects Agency 1400 Wilson Blvd Arlington VA 22209		12. REPORT DATE January 1977
14. MONITORING AGENCY NAME & ADDRESS (if different from Controlling Office) Rome Air Development Center (OCTM) Griffiss AFB NY 13441		13. NUMBER OF PAGES 58
		15. SECURITY CLASS. (of this report) UNCLASSIFIED
		15a. DECLASSIFICATION DOWNGRADING SCHEDULE N/A
16. DISTRIBUTION STATEMENT (of this Report) Approved for public release; distribution unlimited.		
17. DISTRIBUTION STATEMENT (of the abstract entered in Block 20, if different from Report) Same		
18. SUPPLEMENTARY NOTES RADC Project Engineer: Robert F. Ogrodnik (OCTM)		
19. KEY WORDS (Continue on reverse side if necessary and identify by block number) Propagation Turbulence Adaptive Optics Scintillation Speckles		
20. ABSTRACT (Continue on reverse side if necessary and identify by block number) A complete theory is presented for the statistical effects of atmospheric turbulence on coherent radiation reflected from a diffuse target. This study, which is motivated by the need to understand speckle and scintillation effects on the operation of coherent adaptive optical transmitter (COAT) systems, constitutes a significant advance in the field of turbulence scattering phenomena. Both phase and amplitude perturbations are taken into account, and the analysis		

DD FORM 1 JAN 73 1473 EDITION OF 1 NOV 65 IS OBSOLETE

UNCLASSIFIED

SECURITY CLASSIFICATION OF THIS PAGE (When Data Entered)

includes multiple scattering (saturation) conditions and finite receiver apertures. The development is free from certain restrictive assumptions employed in previous work, and yields results for the variance and covariance of irradiance which lead to clear physical insight. It is found that the covariance comprises two additive terms which represent respectively: (1) the incoherent scattering mechanism which is independent of source spectral width, and (2) the coherent mechanism related to "speckles". A technique is also developed for quantitative numerical predictions using reasonable computer time. Results from an ongoing program of experimental verification are given which support the theory.

The effects of nonideal lasers and diffuse targets are discussed briefly, including glints, finite spectral widths, and truncated target regions. It is found that a small diffuse target (or region on a complex target) can give rise under strong turbulence conditions to scintillations with a large normalized irradiance (3), thus constituting a very strong fading mechanism.

UNCLASSIFIED

PROPAGATION OF MULTIWAVELENGTH LASER RADIATION
THROUGH ATMOSPHERIC TURBULENCE

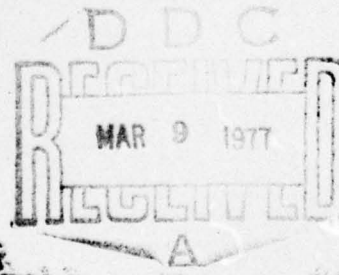
J. Richard Kerr
Richard A. Elliott
Michael E. Fossey
J. Fred Holmes
Myung H. Lee
Philip A. Pincus

Contractor: Oregon Graduate Center
Contract Number: F30602-74-C-0082
Effective Date of Contract: 1 December 1973
Contract Expiration Date: 30 December 1976
Short Title of Work: Propagation of Multi
Wavelength Laser
Radiation
Program Code Number: 6E20
Period of Work Covered: Feb 76 - Nov 76

Principal Investigator: Dr. J. Richard Kerr
Phone: 503 645-1121
Project Engineer: Robert F. Ogrodnik
Phone: 315 330-4306

Approved for public release;
distribution unlimited.

This research was supported by the Defense Advanced
Research Projects Agency of the Department of
Defense and was monitored by Robert F. Ogrodnik (OCTM),
Griffiss AFB NY 13441 under Contract F30602-74-C-0082.



BEST AVAILABLE COPY

This report has been reviewed by the RADC Information Office (OI) and is releasable to the National Technical Information Service (NTIS). At NTIS it will be releasable to the general public, including foreign nations.

This report has been reviewed and approved for publication.

APPROVED:

Robert F. Ogradnik
ROBERT F. OGRADNIK
Project Engineer

Do not return this copy. Retain or destroy.

Summary

A complete theory is presented for the statistical effects of atmospheric turbulence on coherent radiation reflected from a diffuse target. This study, which is motivated by the need to understand speckle and scintillation effects on the operation of coherent adaptive optical transmitter (COAT) systems, constitutes a significant advance in the field of turbulence scattering phenomena.

Both phase and amplitude perturbations are taken into account, and the analysis includes multiple scattering (saturation) conditions and finite receiver apertures. The development is free from certain restrictive assumptions employed in previous work, and yields results for the variance and covariance of irradiance which lead to clear physical insight. It is found that the covariance comprises two additive terms which represent respectively: (1) the incoherent scattering mechanism which is independent of source spectral width, and (2) the coherent mechanism related to "speckles." A technique is also developed for quantitative numerical predictions using reasonable computer time. Results from an ongoing program of experimental verification are given which support the theory.

The effects of nonideal lasers and diffuse targets are discussed briefly, including glints, finite spectral widths, and truncated target regions. It is found that a small diffuse target (or region on a complex target) can give rise under strong turbulence conditions to scintillations with a large normalized irradiance (3), thus constituting a very strong fading mechanism.

CLASSIFIED BY	
EXEMPT	EXEMPT CODED <input checked="" type="checkbox"/>
EXEMPT	EXEMPT CODED <input type="checkbox"/>
CLASSIFIED	CLASSIFIED <input type="checkbox"/>
CLASSIFICATION	
BY	
DISTRIBUTION/AVAILABILITY CODES	
Dist.	AVAIL. and/or SPECIAL
A	

Table of Contents

	<u>Page</u>
Summary	1
I. Introduction	3
II. Analytical Description	4
IIA. Basic Statistics of Speckles Through Turbulence	4
1. Mean Irradiance	4
2. Mutual Coherence Function	7
3. Covariance and Variance	10
4. Incoherent Case	15
5. Receiver Smoothing	15
6. Higher Moments and Probability Distribution of Irradiance	17
7. Physical Interpretation of Variance and Covariance	20
8. Time-Lagged Covariance	26
IIB. Complex Targets and Sources	27
1. Target Truncation	27
2. Glints	31
3. Nonideal Sources	31
III. Numerical Evaluations	32
IIIA. Basic Technique	33
IIIB. Variance of Irradiance	34
IIIC. Covariance of Irradiance	35
IV. Experimental Results	35
IVA. Introduction	35
IVB. Variance Measurements	37
IVC. Covariance Measurements	38
IVD. Other Properties of the Irradiance	39
V. References	40

I. Introduction

This report extends the work described in Ref. 1 involving the statistics of a scintillating field from a laser-illuminated, diffuse target in turbulence. In particular, the significantly restrictive assumptions of the earlier treatment have been dropped, and clear physical interpretations of the resulting complete theory are presented.

The basic analysis, interpretation, and ancillary theoretical considerations are given in Sec. II, followed in Sec. III by a numerical technique for quantitative predictions using moderate computer time. In Sec. IV, supporting experimental efforts are described.

-
1. J. R. Kerr, et al, Propagation of Multiwavelength Laser Radiation Through Atmospheric Turbulence, RADC-TR-76-111, April, 1976, (A024863).

II. Analytical Description

In Sec. II-A we present the complete analysis of the basic statistical properties of irradiance after reflection from a diffuse target in atmospheric turbulence. In II-B we briefly treat further topics such as glints and other considerations relating to the characteristics of real lasers and targets.

As in the preceding report,¹ the treatment utilizes the extended Huygens-Fresnel principle, and includes the effects of turbulence on both the path from the transmitter to the target and that from the target to the receiver (Figure 1). Unless otherwise stated, a TEM₀₀ laser is assumed, with a perfectly diffuse target. Any assumptions are clearly stated as they are introduced; basically however the treatment is quite general and not significantly limited by assumptions such as were utilized in previously reported work.

II-A. Basic Statistics of Speckles Through Turbulence

1. Mean Irradiance

Referring to Figure 1, we assume that the source and target are much smaller than the path length (L), and that the distance between the receiver and source is greater than the source size such that outgoing and incoming radiation experiences independent turbulent regions. The latter limitation is thought to be inessential owing to the diffuse target characteristics, and is under further study.

We write the source amplitude distribution as

$$U_o(\bar{r}) = U_o \exp \left(-\frac{r^2}{2\alpha_o^2} - \frac{ikr^2}{2F} \right) \quad (1)$$

where α_o and F are the characteristic beam radius and focal length respectively. The field at the target is written from the extended

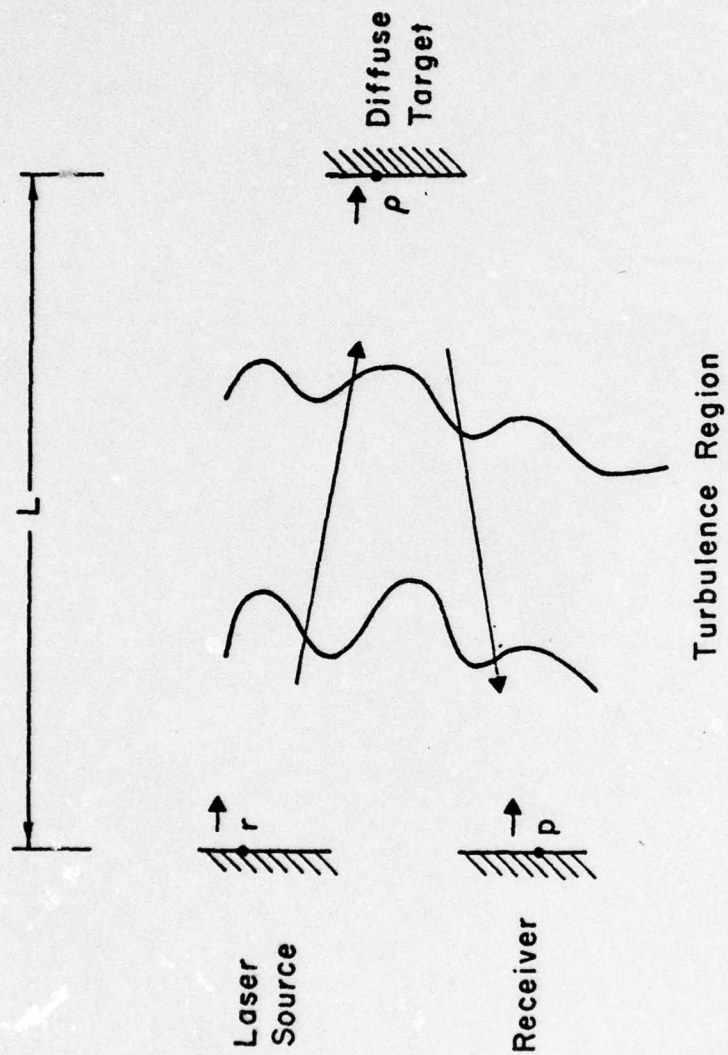


Figure 1. Illuminator, Target, and Receiver Configuration

Huygens-Fresnel principle^{2,3} as

$$U(\bar{\rho}) = \frac{ke^{ikL}}{2\pi iL} \int U_0(\bar{r}) \exp \left[\frac{ik|\bar{\rho} - \bar{r}|^2}{2L} + \psi_1(\bar{\rho}, \bar{r}) \right] d\bar{r} \quad (2)$$

where ψ_1 describes the effects of the random medium on the propagation of a spherical wave. Combining Eqs. (1) and (2), we have

$$U(\bar{\rho}) = \frac{ke^{ik \left[L + \frac{\rho^2}{2L} \right]}}{2\pi iL} U_0 \int \exp \left[-\frac{r^2}{2\alpha_0^2} + \frac{ik}{2L} \left(1 - \frac{L}{F} \right) r^2 - \frac{ik}{L} \bar{\rho} \cdot \bar{r} + \psi_1(\bar{\rho}, \bar{r}) \right] d\bar{r} \quad (3)$$

In particular, this applies to the special cases of a focused ($L = F$) or collimated ($F \rightarrow \infty$) beam respectively.

The field at the receiver is written by reapplying the Huygens-Fresnel principle to the field at the target:

$$U(\bar{\rho}) = \frac{ke^{ik \left[L + \frac{\rho^2}{2L} \right]}}{2\pi iL} \int U'(\bar{\rho}) \exp \left[\frac{ik}{2L} (\rho^2 - 2\bar{\rho} \cdot \bar{\rho}) + \psi_2(\bar{\rho}, \bar{\rho}) \right] d\bar{\rho} \quad (4)$$

where $U'(\bar{\rho})$ is the field solution after reflection from the target, and ψ_2 represents the turbulence effect from the target to the receiver. The mean intensity at the receiver is then

$$\begin{aligned} \langle I(\bar{\rho}) \rangle &= \langle |U(\bar{\rho})|^2 \rangle = \left(\frac{k}{2\pi L} \right)^2 \iint d\bar{\rho}_1 d\bar{\rho}_2 \langle U'(\bar{\rho}_1) U'^*(\bar{\rho}_2) \rangle \\ &\cdot \exp \left[\frac{ik}{2L} ((\rho_1^2 - \rho_2^2) - 2\bar{\rho} \cdot (\bar{\rho}_1 - \bar{\rho}_2)) \right] \\ &\cdot \langle \exp [\psi_2(\bar{\rho}, \bar{\rho}_1) + \psi_2^*(\bar{\rho}, \bar{\rho}_2)] \rangle \end{aligned} \quad (5)$$

2. R. F. Lutomirski and H. T. Yura, "Propagation of a Finite Optical Beam in an Inhomogeneous Medium," *Applied Optics*, 10, 1652, July 1971.
3. H. Yura, "Mutual Coherence Function of a Finite Cross Section Optical Beam Propagating in a Turbulent Medium," *Applied Optics*, 11, 1399, June 1972.

Through the assumption of a diffuse target, the reflected beam suffers a random phase delay from point-to-point over the target, so that

$$\langle U'(\bar{\rho}_1)U'^*(\bar{\rho}_2) \rangle = \langle I(\bar{\rho}_1) \rangle \delta(\bar{\rho}_1 - \bar{\rho}_2) \cdot \frac{4\pi}{k^2} \quad (6)$$

The factor $4\pi/k^2$ requires comment. The dimensions of the δ -function are $(\text{area})^{-1}$, and this factor reflects the correlation which actually exists over a finite area of order k^{-2} . The numerical value 4π is discussed in Ref. 4, and verified below by an independent approach. Using this in Eq. (5), the mean intensity becomes

$$\langle I(\bar{\rho}) \rangle = \frac{1}{\pi L^2} \int d\bar{\rho}_1 \langle |U(\bar{\rho}_1)|^2 \rangle \langle \exp [\psi_2(\bar{\rho}, \bar{\rho}_1) + \psi_2^*(\bar{\rho}, \bar{\rho}_1)] \rangle \quad (7)$$

where the mean exponential term is unity from considerations of energy conservation.³ The resultant mean intensity at the receiver is then simply

$$\langle I(\bar{\rho}) \rangle = \frac{1}{\pi L^2} \int d\bar{\rho} \langle |U(\bar{\rho})|^2 \rangle \quad (8)$$

To complete the solution, we use Eq. (3) with Eq. (8). We note that the structure function gives us ($r = |\bar{r}_1 - \bar{r}_2|$)

$$\langle \exp [\psi_1(\bar{\rho}, \bar{r}_1) + \psi_1^*(\bar{\rho}, \bar{r}_2)] \rangle = e^{-\left(\frac{r}{\rho_0}\right)^{5/3}} \quad (9)$$

For the focused beam, we then have

$$\langle |U(\bar{\rho})|^2 \rangle = \left(\frac{k}{2\pi L}\right)^2 U_0^2 \iint d\bar{r}_1 d\bar{r}_2 \exp \left[-\frac{r_1^2 + r_2^2}{2\alpha_0^2} - \frac{ik}{L} \bar{\rho} \cdot (\bar{r}_1 - \bar{r}_2) - \left(\frac{r}{\rho_0}\right)^{5/3} \right] \quad (10)$$

4. M.J. Beran and G.B. Parrent, Jr., Theory of Partial Coherence, Prentice-Hall, Englewood Cliffs, N.J., 1964.

This describes a target-spot of size $\approx \frac{L}{k\alpha_0}$ or $\frac{L}{k\rho_0}$, for α_0, ρ_0 smaller respectively. Carrying out the integration indicated in Eq. (8), involving the Fourier-Bessel integral, we have finally

$$\langle I(\bar{p}) \rangle = U_0^2 \frac{\alpha_0^2}{L^2} \quad (11)$$

The result for the collimated beam is identical, and in fact could be deduced for an arbitrary beam focus through conservation of energy, as follows. For Lambertian scattering into a hemisphere, the on-axis irradiance at a distance L from the target is

$$\begin{aligned} I &= \frac{\text{Total Power on Target}}{\pi L^2} \\ &= \frac{\int d\bar{r} \langle |U(\bar{r})|^2 \rangle}{\pi L^2} \end{aligned} \quad (12)$$

From Eq. (1), we have

$$\begin{aligned} \int d\bar{r} \langle |U(\bar{r})|^2 \rangle &= U_0^2 \int_0^\infty r dr e^{-r^2/\alpha_0^2} \\ &= U_0^2 \alpha_0^2 \pi \end{aligned} \quad (13)$$

Combining these,

$$I = \frac{U_0^2 \alpha_0^2}{L^2} \quad (14)$$

in agreement with Eq. (11). Thus the (small-angle) mean irradiance at the receiver (illuminator) plane is uniform and independent of turbulence level.

2. Mutual Coherence Function

The mutual coherence function (MCF) may be very important in analyzing the operation of a coherent optical adaptive system, and can be readily derived with the simple assumption of a diffuse target. We write

$$\begin{aligned} \Gamma(\bar{p}_1, \bar{p}_2) &= \left(\frac{k}{2\pi L} \right)^2 \iint d\bar{\rho}_1 d\bar{\rho}_2 \langle U(\bar{\rho}_1) U^*(\bar{\rho}_2) \rangle \exp \left\{ i k \left[R_1(\bar{\rho}_1, \bar{p}_1) \right. \right. \\ &\quad \left. \left. - R_2(\bar{\rho}_2, \bar{p}_2) \right] \right\} \langle \exp \left[\psi_2(\bar{p}_1, \bar{\rho}_1) + \psi_2^*(\bar{p}_2, \bar{\rho}_2) \right] \rangle \end{aligned} \quad (15)$$

where $R_1(\bar{\rho}_1, \bar{p}_1)$, $R_2(\bar{\rho}_2, \bar{p}_2)$ are the distances from $\bar{\rho}_1$ to \bar{p}_1 and $\bar{\rho}_2$ to \bar{p}_2 respectively.

By the Fresnel approximation

$$R_1(\bar{\rho}_1, \bar{p}_1) - R_2(\bar{\rho}_2, \bar{p}_2) \approx \frac{p_1^2 - p_2^2 + \rho_1^2 - \rho_2^2}{2L} - \frac{\bar{p}_1 \cdot \bar{\rho}_1 - \bar{p}_2 \cdot \bar{\rho}_2}{L} \quad (16)$$

Hence, from (15) and (16),

$$\begin{aligned} \Gamma(\bar{p}_1, \bar{p}_2) &= \left(\frac{k}{2\pi L} \right)^2 \exp \left[\frac{ik(p_1^2 - p_2^2)}{2L} \right] \iint d\bar{\rho}_1 d\bar{\rho}_2 \langle U(\bar{\rho}_1) U^*(\bar{\rho}_2) \rangle \\ &\cdot \exp \left\{ ik \left(\frac{\rho_1^2 - \rho_2^2}{2L} - \frac{\bar{p}_1 \cdot \bar{\rho}_1 - \bar{p}_2 \cdot \bar{\rho}_2}{L} \right) \right\} \cdot \exp \left[\psi_2(\bar{p}_1, \bar{\rho}_1) + \psi_2^*(\bar{p}_2, \bar{\rho}_2) \right] \end{aligned} \quad (17)$$

Since the wave is incoherent after reflection from the diffuse target, the coherence function at that plane can again be represented by the Dirac delta function as given in (6). Using this in (17), $\Gamma(\bar{p}_1, \bar{p}_2)$ can be simplified to

$$\begin{aligned} \Gamma(\bar{p}_1, \bar{p}_2) &= \frac{1}{\pi L^2} \exp \left[\frac{ik(p_1^2 - p_2^2)}{2L} \right] \int d\bar{\rho} \langle I(\bar{\rho}) \rangle \exp \left\{ - \frac{ik}{L} (\bar{p}_1 - \bar{p}_2) \cdot \bar{\rho} \right\} \\ &\cdot e^{-\left(\frac{p}{p_0} \right)^{5/3}} \end{aligned} \quad (18)$$

In the absence of turbulence, this equation is entirely identical to the Van Cittert-Zernike theorem of coherence theory,⁵ which is identical to a result obtained by Goodman for the mutual coherence function of a pulsed optical radar.⁶

-
5. M. Born and E. Wolf, Principles of Optics, Pergamon Press, New York, 1975.
 6. J. W. Goodman, "Some Effects of Target-Induced Scintillation on Optical Radar Performance," Proc. IEEE, 53, 1688, 1965.

To complete the solution, we utilize the mean intensity at the target. For the focused case, Eq. (10) may be integrated to yield

$$\langle I(\bar{\rho}) \rangle = \left(\frac{k}{L}\right)^2 |U_0|^2 \frac{\alpha_0^2}{2} \int_0^\infty r dr J_0\left(\frac{k}{L} \rho r\right) e^{-\frac{r^2}{4\alpha_0^2} - \left(\frac{r}{\rho_0}\right)^{5/3}} \quad (19)$$

We thus have

$$\begin{aligned} \Gamma(p_1, p_2) &= \frac{1}{\pi L^2} \left(\frac{k}{L}\right)^2 |U_0|^2 \frac{\alpha_0^2}{2} \int d\bar{\rho} \int_0^\infty r dr J_0\left(\frac{k}{L} \rho r\right) \\ &\quad \cdot e^{-\frac{r^2}{4\alpha_0^2} - \left(\frac{r}{\rho_0}\right)^{5/3}} \exp\left[-\frac{ik}{L} \bar{\rho} \cdot \bar{p} - \left(\frac{\bar{p}}{\rho_0}\right)^{5/3}\right] \\ &\quad \cdot \exp\left[\frac{ik(p_1^2 - p_2^2)}{2L}\right] \\ &= |U_0|^2 \frac{\alpha_0^2 k^2}{L^4} \int_0^\infty \rho d\rho \int_0^\infty r dr J_0\left(\frac{k}{L} \rho r\right) J_0\left(\frac{k}{L} \rho p\right) \\ &\quad \cdot e^{-\frac{r^2}{4\alpha_0^2} - \left(\frac{r}{\rho_0}\right)^{5/3} - \left(\frac{\rho}{\rho_0}\right)^{5/3} + \frac{ik}{2L} (p_1^2 - p_2^2)} \end{aligned} \quad (20)$$

from the Fourier-Bessel integral formula,

$$\int_0^\infty \rho J_0\left(\frac{k}{L} \rho r\right) J_0\left(\frac{k}{L} \rho p\right) d\rho = \left(\frac{L}{k}\right)^2 \frac{1}{\sqrt{rp}} \delta(r-p) \quad (21)$$

Equation (20) can then be simplified and becomes

$$\begin{aligned} \Gamma(\bar{p}_1, \bar{p}_2) &= |U_0|^2 \frac{\alpha_0^2}{L^2} e^{-\frac{p^2}{4\alpha_0^2} - 2\left(\frac{p}{\rho_0}\right)^{5/3} + \frac{ik}{2L} (p_1^2 - p_2^2)} \\ \text{focused} &\quad \cdot e^{-\frac{p^2}{4\alpha_0^2} - 2\left(\frac{p}{\rho_0}\right)^{5/3} + \frac{ik}{2L} (p_1^2 - p_2^2)} \\ &= \langle I(p) \rangle e \end{aligned} \quad (22)$$

Using $\langle I(\bar{\rho}) \rangle$ for the collimated case in (18) and simplifying yields

$$\Gamma(\bar{\rho}_1, \bar{\rho}_2) = \langle I(\bar{\rho}) \rangle e^{-p^2 \left[\left(\frac{1}{2a_0} \right)^2 + \left(\frac{k a_c}{2L} \right)^2 \right] - 2 \left(\frac{p}{\rho_c} \right)^{5/3} + \frac{ik}{2L} (p_1^2 - p_2^2)} \quad (23)$$

Collimated

It may be noted that the MCF's of Eqs. (22) and (23) imply a "white" or constant spatial power spectrum for the (complex) amplitude, resulting from the assumption of a diffuse target. The more interesting spectrum, however, is that of the irradiance, as discussed below.

3. Covariance and Variance

The covariance of irradiance at the receiver is given by

$$C_I(\bar{\rho}_1, \bar{\rho}_3) = \langle I(\bar{\rho}_1) I(\bar{\rho}_3) \rangle - \langle I(\bar{\rho}_1) \rangle \langle I(\bar{\rho}_3) \rangle \quad (24)$$

The first term, the correlation function, is in turn given by the extended Huygens-Fresnel principle as

$$B_I(\bar{\rho}_1, \bar{\rho}_3) = \left(\frac{k}{2\pi L} \right)^4 \iiint d\bar{\rho}_1 d\bar{\rho}_2 d\bar{\rho}_3 d\bar{\rho}_4 \langle U(\bar{\rho}_1) U^*(\bar{\rho}_2) U(\bar{\rho}_3) U^*(\bar{\rho}_4) \rangle \cdot \exp[ik(R_1 - R_2 + R_3 - R_4)] H(\bar{\rho}_1, \bar{\rho}_2, \bar{\rho}_3, \bar{\rho}_4; \bar{\rho}_1, \bar{\rho}_3) \quad (25)$$

where H is the fourth order mutual coherence function given by

$$H = \langle \exp[\psi(\bar{\rho}_1, \bar{\rho}_1) + \psi^*(\bar{\rho}_2, \bar{\rho}_1) + \psi(\bar{\rho}_3, \bar{\rho}_3) + \psi^*(\bar{\rho}_4, \bar{\rho}_3)] \rangle \quad (26)$$

and

$$R_1 = |\bar{\rho}_1 - \bar{\rho}_1|$$

$$R_2 = |\bar{\rho}_1 - \bar{\rho}_2|$$

$$R_3 = |\bar{\rho}_3 - \bar{\rho}_3|$$

$$R_4 = |\bar{\rho}_3 - \bar{\rho}_4|$$

After reflection from the diffuse target, the fields are Gaussian and spatially incoherent.* Therefore, the fields at the target can be expressed as

$$\begin{aligned}
 \langle U(\bar{\rho}_1)U^*(\bar{\rho}_2)U(\bar{\rho}_3)U^*(\bar{\rho}_4) \rangle &= \langle U(\bar{\rho}_1)U^*(\bar{\rho}_2) \rangle \langle U(\bar{\rho}_3)U^*(\bar{\rho}_4) \rangle \\
 &+ \langle U(\bar{\rho}_1)U^*(\bar{\rho}_4) \rangle \langle U^*(\bar{\rho}_2)U(\bar{\rho}_3) \rangle \\
 &= \langle I(\bar{\rho}_1) \rangle \langle I(\bar{\rho}_3) \rangle \delta(\bar{\rho}_1 - \bar{\rho}_2) \delta(\bar{\rho}_3 - \bar{\rho}_4) \cdot \left(\frac{4\pi}{k^2}\right)^2 \\
 &+ \langle I(\bar{\rho}_1) \rangle \langle I(\bar{\rho}_3) \rangle \delta(\bar{\rho}_1 - \bar{\rho}_4) \delta(\bar{\rho}_3 - \bar{\rho}_2) \cdot \left(\frac{4\pi}{k^2}\right)^2 \quad (27)
 \end{aligned}$$

We use this in Eq. (25), and also utilize Eqs. (A9,A10) from Appendix A to yield

$$\begin{aligned}
 B_1(\bar{p}_1, \bar{p}_3) &= \frac{1}{\pi^2 L^4} \iint d\bar{\rho}_1 d\bar{\rho}_3 \langle I(\bar{\rho}_1) \rangle \langle I(\bar{\rho}_3) \rangle e^{4C_x(\bar{p}_1 - \bar{p}_3, \bar{\rho}_1 - \bar{\rho}_3)} \\
 &+ \frac{1}{\pi^2 L^4} \iint d\bar{\rho}_1 d\bar{\rho}_3 \langle I(\bar{\rho}_1) \rangle \langle I(\bar{\rho}_3) \rangle \exp \left\{ \frac{ik}{L} (\bar{z}_3 - \bar{z}_1) \cdot (\bar{p}_1 - \bar{p}_3) \right\} \\
 &\cdot H(\bar{\rho}_1 - \bar{\rho}_3, \bar{p}_1 - \bar{p}_3) \quad (28)
 \end{aligned}$$

where use has been made of

$$\begin{aligned}
 R_1 - R_2 &\simeq \frac{1}{2L} \left[\rho_1^2 - \rho_2^2 - 2(\bar{\rho}_1 - \bar{\rho}_2) \cdot \bar{p}_1 \right] \\
 R_3 - R_4 &\simeq \frac{1}{2L} \left[\rho_3^2 - \rho_4^2 - 2(\bar{\rho}_3 - \bar{\rho}_4) \cdot \bar{p}_3 \right]
 \end{aligned}$$

*This assumes that the total power contributing to the reflected field at any point is substantially constant, a condition which is satisfied in the present case of an extended target which intercepts the entire transmitted beam.

We now combine (8), (24), and (28) to give ($\bar{p} \equiv \bar{p}_1 - \bar{p}_3$, $\bar{\rho} \equiv \bar{\rho}_1 - \bar{\rho}_3$):

$$c_I(\bar{p}) = \frac{1}{\pi^2 L^4} \iint d\bar{\rho}_1 d\bar{\rho}_3 \langle I(\bar{\rho}_1) \rangle \langle I(\bar{\rho}_3) \rangle \cdot \left[\left(e^{4C_X(\bar{p}, \bar{\rho})} - 1 \right) + e^{-(ik/L)\bar{p} \cdot \bar{\rho}} H(\bar{\rho}, \bar{p}) \right] \quad (29)$$

where H is given by Eq. (A11). This is a very important result, and represents a crucial extension of the developments of the preceding report. In particular, the first term $\left(e^{4C_X(\bar{p}, \bar{\rho})} - 1 \right)$ was not included in the earlier analysis (cf. Eq. 76, Ref. 1) and represents the "incoherent" contribution to the covariance. This contribution is that which would be present in the temporally incoherent-source case (Sec. II-A4) and arises from the log-amplitude perturbation alone. In contrast, the remaining "coherent" term (H) involves both phase and amplitude perturbations multiplicatively (Eq. A11) and vanishes in the incoherent-source case.

The incoherent term will be seen later to involve covariance scales related to the "source"* size and $\sqrt{L/k}$, while the coherent term basically involves the ρ_0 ("atmospheric") and free space ("target") speckle scales. Since the incoherent and coherent terms are additive, there will be correlation over the scales of the incoherent term even when the coherent speckles become small, as is observed in the experiments reported in a later section. That is, the presence of small, high-contrast speckles will not obviate larger correlation scales which would be present regardless of the temporal coherence of the source.

We note that $H(\bar{\rho}, \bar{p})$ involves both phase and amplitude perturbations, with the form of the latter strongly dependent on the strength of scattering for a point source over the path (Appendix A). We will accordingly distinguish "weak" and "saturated" (multiple scattering) conditions.

To further reduce Eq. (29), we utilize Eq. (10) for the focused case,

*The "source" will hereafter refer to the spot on the target.

and tedious but straightforward integrations. The result is

$$C_I(\bar{p}) = \frac{2}{\pi} \frac{k^2}{L^2} |U_0|^4 \left(\frac{\alpha_0^2}{2} \right)^2 \int_0^\infty r dr e^{-r^2/2\alpha_0^2 - 2(r/\rho_0)^{5/3}} \\ \times \int d\bar{\rho} J_0 \left(\frac{k}{L} r \rho \right) \left[\left(e^{4C_X(\bar{p}, \bar{\rho})} - 1 \right) + e^{-(ik/L)\bar{p} \cdot \bar{\rho}} H(\bar{p}, \bar{\rho}) \right] \quad (30)$$

The corresponding result for an arbitrary focus is obtained by inserting

$$\exp \left\{ -r^2 \frac{k^2}{2L^2} \alpha_0^2 \left(1 - \frac{L}{F} \right)^2 \right\} \text{ in the first integral. This substitution}$$

is appropriate in all similar expressions in the remainder of the report, so that the discussion can be confined to the focused beam case without loss of generality.

These results (30) are five-fold integrals but not formidable; their physical interpretation and numerical evaluation will be discussed further in later sections.

The variance, normalized by the square of the mean irradiance, is given by Eqs. (30) and (A12):

$$C_{In}^2 = \frac{C_I(0)}{U_0^4 \alpha_0^4 / L^4} = \frac{k^2}{L^2} \int_0^\infty r dr e^{-r^2/2\alpha_0^2 - 2(r/\rho_0)^{5/3}} \\ \times \int \rho d\rho J_0 \left(\frac{k}{L} r \rho \right) \left[2e^{4C_X(\bar{\rho})} - 1 \right] \quad (31)$$

In order to identify the incoherent and coherent contributions respectively, the final bracket may be written

$$\left[\left(e^{4C_X(\bar{\rho})} - 1 \right) + e^{4C_X(\bar{\rho})} \right]$$

It is of interest to compare this variance result with that obtained in the preceding report under the assumption that phase perturbations dominate. In that case, the normalized variance was found to be identically unity. From the present complete analysis, we see that the phase perturbations do not explicitly enter the variance expression, the phase having been totally randomized by the diffuse target. In the limit of weak turbulence ($C_x = 0$), the integrations in Eq. (31) will yield a variance of unity, physically owing to the diffuse target (free-space speckles); in the limit of strong turbulence, it will also be unity ($C_x = 0$ for $\rho > \rho_0 = \epsilon$, where ϵ is vanishingly small). For intermediate values of turbulence, the variance will be somewhat greater than unity, as a result of non-negligible amplitude perturbations (C_x). These physical interpretations will be discussed in detail in a later section.

We may often assume in Eqs. (30,31) that $4C_x \ll 1$, so that $(2e^{4C_x} - 1) \approx 1 + 8C_x$. This is a good approximation in weak turbulence and a rough but useful approximation in strong turbulence, and may substantially simplify further analysis. For example, Eq. (31) with (A4) becomes

$$\sigma_{I_n}^2 \approx 1 + 1.06 \pi^2 k^2 C_n^2 L \int_0^1 dt \int_0^\infty du u^{-8/3} \times \exp \left\{ -\frac{1}{2\alpha_0^2} \left[\frac{u}{k} L (1-t) \right]^2 - \frac{2}{\rho_0^{5/3}} \left[\frac{u}{k} L (1-t) \right]^{5/3} \right. \\ \left. \sin^2 \left[\frac{u^2 L t (1-t)}{2k} \right] \right\} \quad (32)$$

For the saturated case, (31) with (A5) yield

$$\sigma_{I_n}^2 \approx 1 + 3.0 \int_0^1 du \int_0^\infty dq e^{-q} - \frac{1}{2} \left(\frac{5.69 u L}{\rho_0 \alpha_0 k} \right)^2 \frac{1}{q^{6/5}} - \frac{2}{q} \left(\frac{5.69 u L}{k \rho_0^2} \right)^{5/3} \quad (33)$$

These expressions clearly show the increment from unity variance related to the log amplitude perturbation. Large values of α_0 and ρ_0 , corresponding to small target spot-size, result in greater variance (stronger scintillations).

4. Incoherent Case

In order to derive the covariance for a temporally incoherent source, we return to Eq. (25) and write

$$B_I(\bar{p}_1, \bar{p}_3) \sim \iiint d\bar{\rho}_1 d\bar{\rho}_2 d\bar{\rho}_3 d\bar{\rho}_4 \iiint dk_1 dk_2 dk_3 dk_4 \\ \cdot \langle U_1(\bar{\rho}_1, k_1) U_2^*(\bar{\rho}_2, k_2) U_3(\bar{\rho}_3, k_3) U_4^*(\bar{\rho}_4, k_4) \rangle \\ \cdot \exp\{i(k_1 R_1 - k_2 R_2 + k_3 R_3 - k_4 R_4)\} \cdot H(\bar{\rho}_1 \cdot \bar{\rho}_4; \bar{p}_1, \bar{p}_3) \quad (34)$$

We then note that the incoherence of the source implies that the integrals over k_{1-4} will yield zero except for $(k_1, \bar{\rho}_1) = (k_2, \bar{\rho}_2)$ and $(k_3, \bar{\rho}_3) = (k_4, \bar{\rho}_4)$. This drops the phase perturbation out of H , by virtue of Eq. (A9), and we are left with

$$B_I(\bar{p}) \sim \iint d\bar{\rho}_1 d\bar{\rho}_3 \langle I(\bar{\rho}_1) \rangle \langle I(\bar{\rho}_3) \rangle \cdot e^{4C_X(\bar{\rho}_3 - \bar{\rho}_1, \bar{p})} \quad (35)$$

The corresponding covariance is then recognized as the "incoherent part" of the general covariance of Eq. (29).

We also point out that this result is easily shown to be consistent with the results of Ref. 7, in which a spatial-frequency domain treatment is given for a target under ambient illumination.

5. Receiver Smoothing

In this section we treat the smoothing of diffuse-target scintillations by a finite receiver aperture.

We define the receiver weighting function as $W(\bar{p}, D)$:

$$W(\bar{p}, D) = \begin{cases} 1 & \text{if } |\bar{p}| \leq \frac{D}{2} \\ 0 & \text{if } |\bar{p}| > \frac{D}{2} \end{cases} \quad (36)$$

7. S. F. Clifford, G. R. Ochs, and Ting-i Wang, "Optical Wind Sensing by Observing the Scintillations of a Random Scene", *Applied Optics*, 14, 2844, December 1975.

The mean, smoothed (aperture-integrated) receiver intensity is simply (Eq.11)

$$\begin{aligned}\langle I_s \rangle &= \int d\bar{p} \, W(\bar{p}, D) \langle I(\bar{p}) \rangle \\ &= \frac{\pi D^2}{4} U_0^2 \frac{\alpha_0^2}{L^2}\end{aligned}\quad (37)$$

The mean-square intensity is

$$\langle I_s^2 \rangle = \iint d\bar{p}_1 d\bar{p}_2 \langle I(\bar{p}_1) I(\bar{p}_2) \rangle W(\bar{p}_1, D) W(\bar{p}_2, D) \quad (38)$$

and the variance is

$$\sigma_{I_s}^2 = \iint d\bar{p}_1 d\bar{p}_2 W(\bar{p}_1, D) W(\bar{p}_2, D) C_I(\bar{p}_1, \bar{p}_2) \quad (39)$$

We let $\bar{p}_1 - \bar{p}_2 = \bar{p}$, $\bar{p}_1 + \bar{p}_2 = 2\bar{p}'$ and integrate over \bar{p}' :

$$\begin{aligned}M(p, D) &\equiv \int d\bar{p}' W(\bar{p}' + \bar{p}/2, D) W(\bar{p}' - \bar{p}/2, D) \\ &= D^2/2 \left\{ \cos^{-1} (p/D) - (p/D) [1 - p^2/D^2]^{1/2} \right\} \text{ if } p \leq D \\ &= 0 \quad \text{if } p > D\end{aligned}$$

Letting $\bar{x} \equiv \bar{p}/D$, we have

$$\sigma_{I_s}^2 = \frac{\pi D^4}{4} \int_{|\bar{x}| \leq 1} d\bar{x} \, M(x) \, C_I(D\bar{x}) \quad (40)$$

With $M(x) = 2/\pi [\cos^{-1} x - x \sqrt{1-x^2}]$

and C_I is given by Eq. (30).

In order to obtain the finite-receiver covariance, we define variables \bar{r}_1, \bar{r}_2 as in Figure 2. Then

$$\begin{aligned}\langle I_{s_1} \rangle &= \int \langle I(\bar{p}_1 + \bar{r}_1) \rangle W(\bar{r}_1) d\bar{r}_1 \\ &= \int \langle I(\bar{p}_2 + \bar{p} + \bar{r}_1) \rangle W(\bar{r}_1) d\bar{r}_1 \\ \langle I_{s_2} \rangle &= \int \langle I(\bar{p}_2 + \bar{r}_2) \rangle W(\bar{r}_2) d\bar{r}_2\end{aligned}\quad (41)$$

and finally

$$C_{I_s}(\bar{p}) = \pi D^4/4 \int_{|\bar{x}| \leq 1} d\bar{x} M(\bar{x}) C_I(\bar{p} + D\bar{x}) \quad (42)$$

6. Higher Moments and Probability Distribution of Irradiance

The phase and amplitude perturbations imply exponential and log normal irradiance statistics respectively. It is of great interest to define the composite probability distribution as a function of the pertinent parameters. Analytical and qualitative considerations will be reviewed in this section; a complete treatment is quite complex and has not yet been accomplished.

We approach the probability distribution through its moments. From Eq. (28), we write the second moment of irradiance as

$$\langle I^2(\bar{p}) \rangle = 2/\pi^2 L^4 \iint d\bar{\rho}_1 d\bar{\rho}_3 \langle I(\bar{\rho}_1) \rangle \langle I(\bar{\rho}_3) \rangle e^{4C_\chi(|\bar{\rho}_1 - \bar{\rho}_3|)} \quad (43)$$

This may be generalized to the n th moment:

$$\langle I^n(\bar{p}) \rangle = n! \left(\frac{1}{\pi L^2} \right)^n \int \dots \int d\bar{\rho}_1 \dots d\bar{\rho}_n \left[\prod_{i=1}^n \langle I(\bar{\rho}_i) \rangle \right] \exp \left[2 \sum_{i \neq j}^n C_{\chi_{ij}} \right] \quad (44)$$

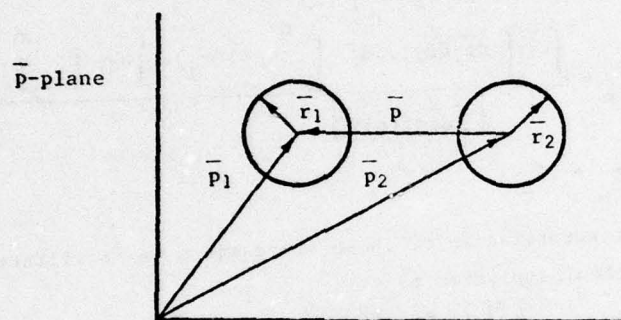


Figure 2. Aperture-Smoothed Covariance: Definition of Variables.

We write this as

$$\langle I^n(\bar{p}) \rangle = n! \langle I(\bar{p}) \rangle^n F_n \quad (45)$$

where

$$\begin{aligned} F_1 &= 1 \\ F_2 &= \frac{\iint d\bar{\rho}_1 d\bar{\rho}_3 \langle I(\bar{\rho}_1) \rangle \langle I(\bar{\rho}_3) \rangle e^{C_X(|\bar{\rho}_1 - \bar{\rho}_3|)}}{\left[\int d\bar{\rho}_1 \langle I(\bar{\rho}_1) \rangle \right]^2} \\ F_n &= \frac{\int \dots \int d\bar{\rho}_1 d\bar{\rho}_2 \dots d\bar{\rho}_n \left[\prod_{i=1}^n \langle I(\bar{\rho}_i) \rangle \right] \exp \left[2 \sum_{i \neq j}^n C_X(|\bar{\rho}_i - \bar{\rho}_j|) \right]}{\left[\int d\bar{\rho} \langle I(\bar{\rho}) \rangle \right]^n} \end{aligned} \quad (46)$$

Note that $\sigma_{I_n}^2 = 2F_2 - 1$.

The interpretation of these expressions is facilitated if we assume $C_X \ll 1$. F_2 then simplifies to

$$F_2 \approx 1 + \frac{4 \iint d\bar{\rho}_1 d\bar{\rho}_3 \langle I(\bar{\rho}_1) \rangle \langle I(\bar{\rho}_3) \rangle C_X(|\bar{\rho}_1 - \bar{\rho}_3|)}{\left[\int d\bar{\rho}_1 \langle I(\bar{\rho}_1) \rangle \right]^2} \quad (47)$$

where the denominator is, from Eq. (19):

$$\left[\int d\bar{\rho}_1 \langle I(\bar{\rho}_1) \rangle \right]^2 = \pi U_o^2 \alpha_o^2 \quad (48)$$

Using Eqs. (10) and (A4), the integral in the numerator of (47) is

$$\begin{aligned} F_2 &\approx 1 + 5.21 C_n^2 k^2 L \int_c^\infty u^{-8/3} du \int_0^1 dt e^{-u^2 L^2 t^2 / 2 \alpha_o^2 k^2 - 2(uLt/k\alpha_o)^{5/3}} \\ &\quad \times \sin^2 [u^2 Lt(1-t)/2k] \end{aligned} \quad (49)$$

For saturated scintillations, Eqs. (10) and (A5) give

$$F_2 \approx 1 + 1.5 \int_0^1 du \int_0^\infty dq \exp \left\{ -q - \frac{1}{2} \left(\frac{5.69 uL}{k\rho_0 \alpha_0} \right)^2 \frac{1}{q^{6/5}} - \frac{2}{q} \left(\frac{5.69 uL}{k\rho_0^2} \right)^{5/3} \right\} \quad (50)$$

We then have the second moment from Eq. (45):

$$\langle I^2(\bar{p}) \rangle = 2 \langle I(\bar{p}) \rangle^2 F_2 \quad (51)$$

and the nth moment is

$$\langle I^n \rangle \approx n! \langle I \rangle^n \left\{ 1 + \frac{n(n-1)}{2} (F_2 - 1) \right\} \quad (52)$$

Hence nonunity F_2 represents the departure from an exponential intensity distribution. Note that F_2 will be unity for weak turbulence ($C_X \approx 0$), or for a large target spot resulting from a small transmitter (small α_0), deliberate defocusing, or strong turbulence (small ρ_0).

Eq. (52) is only a good approximation for n such that $nC_X \ll 1$. It is tempting to derive the probability distribution using (52) with

$$\langle e^{-sI} \rangle = 1 - s \langle I \rangle + \frac{s^2 \langle I^2 \rangle}{2!} - \frac{s^3 \langle I^3 \rangle}{3!} + \dots \quad (53)$$

Defining $\langle I \rangle = I_0$, the result is

$$P_I(I) = \frac{1}{I_0} e^{-I/I_0} \left\{ 1 + (F_2 - 1) \left[1 - \frac{2I}{I_0} + \frac{I^2}{2I_0^2} \right] \right\} + (\text{higher-order terms}) \quad (54)$$

where the "higher-order terms" recognize the limitations on (52). Although this result appears to give a first-order correction to the exponential distribution, it is apparent that the higher moments play a crucial role in the probability distribution since this apparent correction does not agree with physical reasonings.

Specifically, let us take the heuristic viewpoint that the irradiance, at least for small C_X , is comprised of the sum of two random processes, with

exponential and log normal distributions respectively. The composite distribution is given by the convolution of these distributions, with the qualitative effect shown in Figure 3. This prediction agrees with experimental results discussed in Section IV, but not with the expression in (54).

Work is continuing on the derivation of analytic expressions for the probability of irradiance.

7. Physical Interpretation of Variance and Covariance

The physical interpretation of the variance and covariance as expressed in Eqs. (30) and (31) respectively reveals the mechanisms involved in speckle propagation through turbulence in a particularly illuminating manner.

The variance, Eq. (31), may be expressed as

$$\sigma_{In}^2 = 2 e^{4\gamma \sigma_X^2} - 1 \quad (55)$$

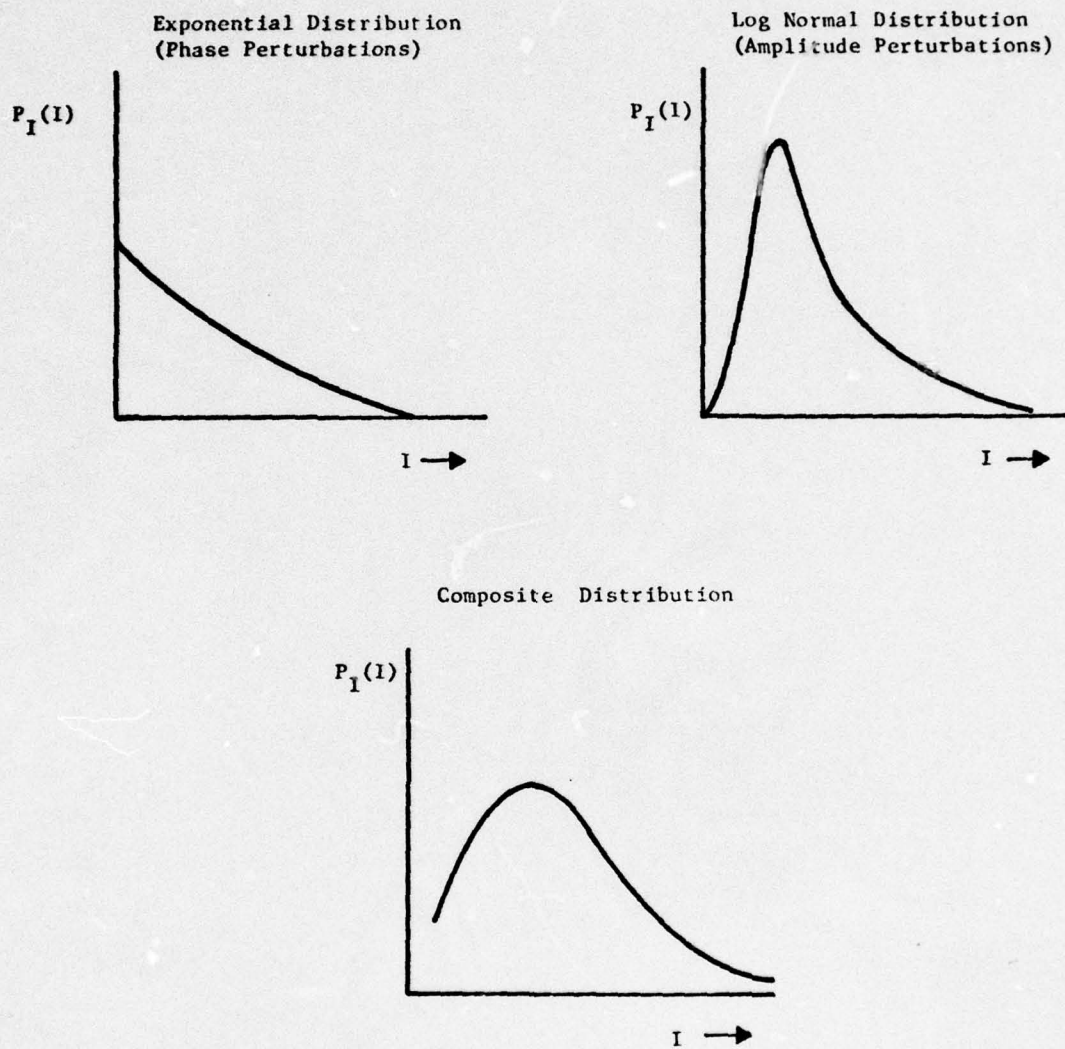
which in many cases can be written

$$\sigma_{In}^2 \approx 1 + 8\gamma \sigma_X^2 \quad (55a)$$

In these expressions, σ_X^2 is the log amplitude variance for a point source propagating over the target-receiver path, and γ (≤ 1) is the "source smoothing factor" associated with the nonzero spot size (S) on the target. Mathematically, γ relates to the integration over (ρ) in Eq. (31), with the spot size ($S = \frac{L}{k\alpha_0}$ or $\frac{L}{k\rho_0}$) coupled through r . For a small transmitter (or defocused spot), or strong turbulence, the target spot will be $S \approx \sqrt{L/k}$ and γ will be less than unity. In the limit of strong turbulence, $\gamma \approx 0$ while for weak turbulence, $\sigma_X^2 = 0$; either extreme results in a unity variance.

A quantitative estimate of γ may be obtained as follows. From published results⁸ for the variance with an extended incoherent source, we know that in weak scattering

8. R. F. Lutomirski, et al, Degradation of Laser Systems by Atmospheric Turbulence, RAND Report R-1171-ARPA/RC, June 1973.



• Figure 3. Qualitative Probability Distribution of Irradiance

$$\gamma \sim \left(\frac{S}{\sqrt{L/k}} \right)^{-7/3} \quad (56a)$$

The smoothing in the strong scattering case is conjectured to be

$$\gamma \sim \left(\frac{S}{\rho_G} \right)^{-2} \quad (56b)$$

This source or target-spot smoothing is analogous to finite-receiver smoothing.⁹

The expressions corresponding to (55) for an incoherent source are (Sec. 11A4):

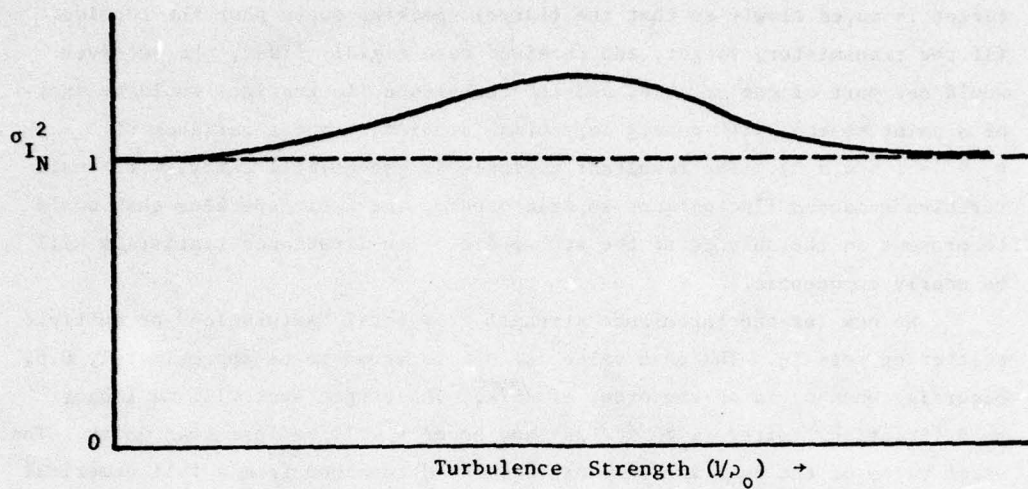
$$\sigma_{I_n}^2 = e^{4\gamma \sigma_X^2} - 1 \quad (57)$$

$$\sigma_{I_n}^2 \sim 4\gamma \sigma_X^2 \quad (57a)$$

It may be seen that the unity baseline and half the remaining term in (55a) arise from the source coherence or speckle phenomenon, whether controlled by the target (weak turbulence) or atmosphere (strong turbulence). Alternatively, we may observe that the unity term arises strictly from phase randomization, with associated exponential irradiance statistics (Ref. 1), while the remaining term represents the effects of nonzero amplitude perturbations, with associated log normal statistics. This supports the heuristic probability arguments of the previous section.

To further illustrate these considerations, let us consider the large, focused transmitter condition ($\alpha_0 \gg \sqrt{L/k}$) (Figure 4). We first consider the weak turbulence condition ($\rho_0 > \alpha_0 > \sqrt{L/k}$), in which the transmitter is able to operate in an essentially diffraction-limited manner. The target-spot is small, i.e. such that the receiver is in the far-field of the spot, and the situation is much like that of a point source ($\sigma_X^2 \ll 1, \gamma=1$). There is however one major difference from the point-source case: we assume a good statistical

9. R. S. Lawrence and J. W. Strohbehn, "A Survey of Clean-Air Propagation Effects Relevant to Optical Communications", Proc. IEEE, 58, 1523, October 1970.



$$\{\rho_0 > \alpha_0 > \sqrt{L/k}\}$$

$$\sigma_X^2 \ll 1$$

$$\gamma = 1$$

$$\{\alpha_0 > \rho_0 \sim \sqrt{L/k}\}$$

$$\sigma_X^2 \sim 0.6$$

$$\gamma < 1$$

$$\{\alpha_0 > \sqrt{L/k} > \rho_0\}$$

$$\sigma_X^2 \sim 0.17$$

$$\gamma \ll 1$$

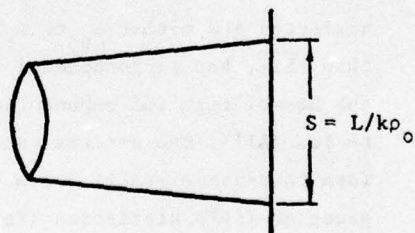
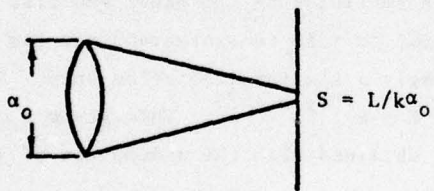


Figure 4. Normalized Variance of Irradiance for Increasing Turbulence

(ensemble) average of the field, which as a practical matter means that the target is moved slowly so that the (large) speckles sweep past the receiver. (If the transmitter, target, and receiver were rigidly fixed, the receiver would see part of one speckle, and the turbulence fluctuations would be that of a point source, with purely log normal statistics and a variance of $e^{4\sigma_X^2} - 1 \sim 4\sigma_X^2$). The resultant variance is essentially unity, with small turbulence-caused fluctuations superimposed on the basic speckles that would be present in the absence of the atmosphere. The irradiance statistics will be nearly exponential.

We now let the turbulence strength grow until "saturation" or multiple scattering sets in. The peak value⁹ of σ_X^2 is known to be approximately 0.6, occurring when ρ_0 is on the order of $\sqrt{L/k}$. The target spot will no longer be diffraction limited ($\alpha_0 > \rho_0 \sim \sqrt{L/k}$), and hence γ will be less than unity. The exact value of the peak variance can only be determined from a full numerical evaluation of Eq. (31), including the detailed effects of saturation on $C_X(\bar{\rho})$; the statistics will be a composite of log normal and exponential distributions. As the turbulence strength grows further, σ_X^2 decreases ("super-saturation") to the limit ~ 0.17 ; also the target-spot grows indefinitely, so that γ decreases to zero in the limit. The variance therefore decreases back to unity (Fig. 4), with exponential statistics.

We now consider the covariance case, again for a focused transmitter.

We refer again to Eq. (30). For the coherent (H) term, if C_X is neglected and either α_0 or ρ_0 is much smaller than the other and also smaller than $\sqrt{L/k}$, the corresponding limitation on r in the integrand couples through the Bessel term and exponential to imply a similar limitation on p . Referring to Eq. (A11), the ρ -terms cancel and $H = e^{-2(p/\rho_0)^{5/3}}$. This gives a closed-form covariance result which is that obtained with the assumption of joint gaussian field statistics (Ref. 1):

$$C_{I_n}(\bar{\rho}) = e^{-p^2/2\alpha_0^2 - 4(p/\rho_0)^{5/3}} \quad (58)$$

Hence the covariance arising from the coherent term in Eq. (30) is generally exponential with a scale equal to the smaller of α_0 or ρ_0 (target and atmos-

pheric speckles respectively). In the event that α_0 and ρ_0 are comparable, the complete expression must be used and the field statistics are marginally (but not joint) gaussian.¹ In the event that C_χ is non-negligible, the covariance scale relating to the coherent term is largely unaffected.

We now consider the incoherent term in (30). If the target spot is small compared to $\sqrt{L/k}$, i.e. α_0 and $\rho_0 \gg \sqrt{L/k}$, the large range of r in the integrand will couple through J_0 to hold ρ small in C_χ . Hence the covariance scale will be determined by $C_\chi(p, 0)$ and will be $\sqrt{L/k}$ as expected for a small target spot. However, for a large target spot (S), the ρ range in the integrand will be large and the p -scale in C_I will be "smeared" to the order of S . This effect is consistent with the incoherent-source results of Ref. 7, and can be argued from simple geometry: for two receivers separated by a small distance relative to the source size, the source-turbulence configuration over the paths to each respective receiver will be highly correlated. The statistics associated with the incoherent term are log normal, although the log amplitude is not joint normal except for weak fluctuations.¹⁰

We now summarize the above reasonings with respect to particular parameter realms:

$$a) \sqrt{L/k} < \alpha_0, \rho_0$$

In this case, the target spot is small, the receiver is in the far field of the spot, and $\gamma = 1$. The covariance contains both a phase and amplitude term as shown in Figure 5a. The amplitude term has a variance contribution of $2(e^{4\sigma_\chi^2} - 1) \sim 8\sigma_\chi^2$ and a scale of $\sqrt{L/k}$, while the phase term has a variance of unity and scale equal to the smaller of (α_0, ρ_0) . The latter scale represents the speckle size, as determined by the target spot size ($L/k\alpha_0$ or $L/k\rho_0$). Region II is dominated by free-space speckles, such that the associated temporal spectrum is determined by target-receiver motion and the statistics* relate to the exponential irradiance distribution. In Region I, the

*These statements regarding statistics related to covariance realms do not necessarily imply joint log normal or joint exponential statistics for two points separated by p , but rather relate to the single-point statistics of the corresponding mechanisms.

10. J. R. Kerr, et al, Propagation of Multiwavelength Laser Radiation Through Atmospheric Turbulence, RADC-TR-76-49, March 1976, (A023202).

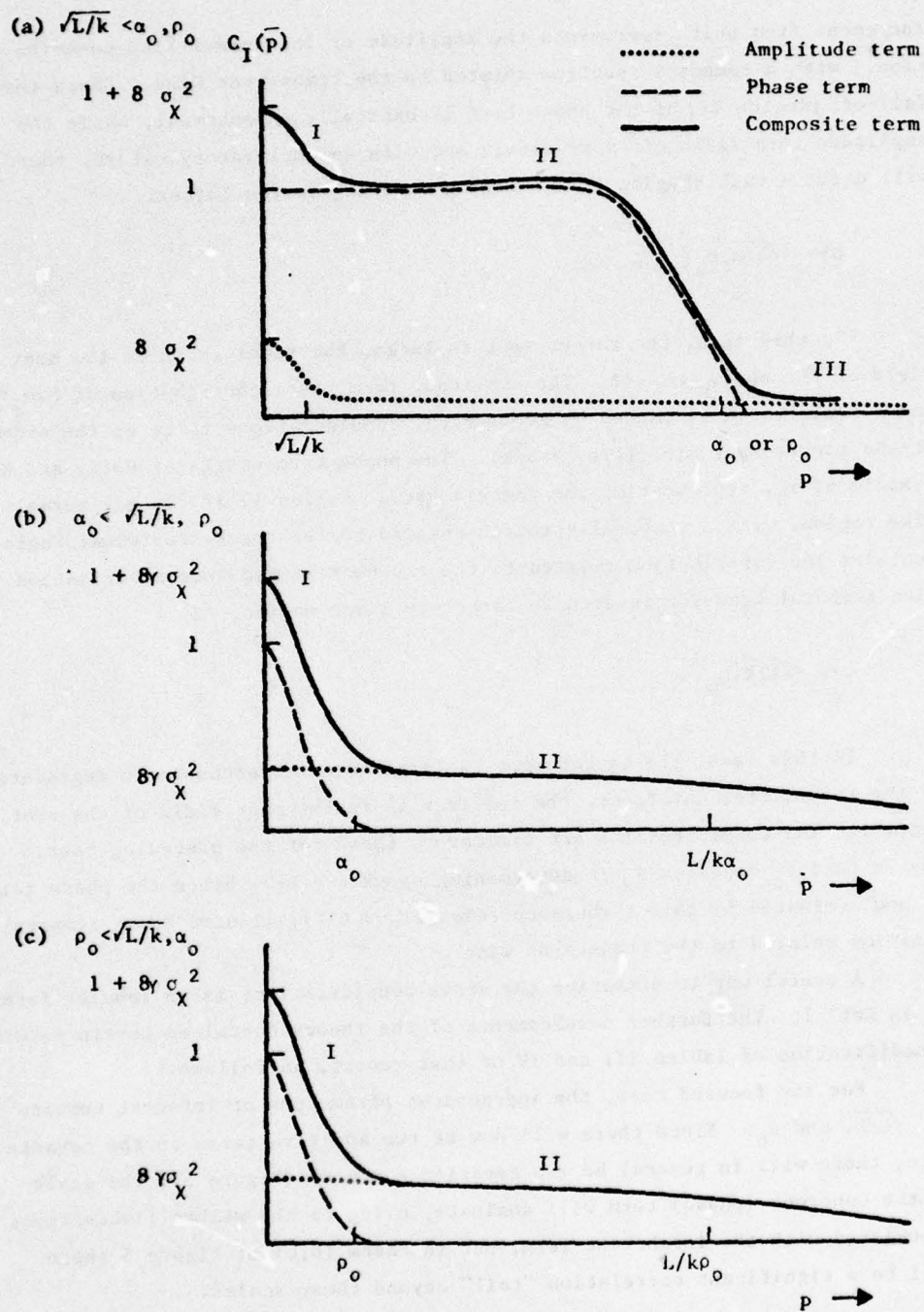


Figure 5. Covariance Curves

increment from unity represents the amplitude or log-normal-like contribution,* with a temporal spectrum related to the transverse wind. Since the fall-off (Region II) of the phase term is basically exponential, while the amplitude term falls off more slowly and with an oscillatory nature, there will exist a tail (Region III) relating entirely to the latter.

$$b) \alpha_0 < \sqrt{L/k}, \rho_0$$

In this case, the target spot is large, the receiver is in the near field of the spot, and $\gamma < 1$. The amplitude term has a contribution of $8\gamma\sigma_x^2$, and a scale which is caused by geometrical considerations to be on the order of the target-spot size ($L/k\alpha_0 > \sqrt{L/k}$). The phase term starts at unity and has a scale of α_0 , representing the speckle size. Region II is the log-normal-like region, with a temporal spectrum related to the transverse wind; Region I includes the contribution related to the exponential radiance distribution, with temporal behavior related to target-receiver motion.

$$c) \rho_0 < \sqrt{L/k}, \alpha_0$$

In this case, the target spot is large owing to atmospheric degradation of the transmitter wavefront, the receiver is in the near field of the spot, and $\gamma < 1$. The considerations are similar to those for the preceding case, except that ρ_0 replaces α_0 in determining speckle size. Since the phase term is now dominated by this turbulence-related quantity, it also has a temporal behavior related to the transverse wind.

A useful way to summarize the above considerations is in tabular form as in Ref. 1. The further developments of the theory contained herein require a modification of Tables III and IV of that report, as follows.

For the focused case, the independent parameters of interest remain α_0 , $\sqrt{L/k}$, and ρ_0 . Since there will now be two additive terms in the covariance, there will in general be two covariance scales (Figure 5); the scale of the coherent (phase) term will dominate, owing to the weaker fluctuations associated with the incoherent term, but in cases (b,c) of Figure 5 there will be a significant correlation "tail" beyond these scales.

The results are given in Table I. In parameter realms A and B, in which the receiver is in the far field of the small target spot, we distinguish two cases. In case 1, we assume strict mechanical stability between the transmitter, target, and receiver, such that the (very large) speckles are not moving. Each receiver will then sample an unvarying, small portion of a speckle and the only fluctuations will be those arising as from a point source in turbulence; this well-known⁹ situation involves a different definition of statistical averaging than that which is implied in the foregoing analysis. In case 2, the ergodic ensemble average is used which corresponds to movement of the speckles past the receiver. As a practical matter, an imperfectly "fixed" target-transceiver configuration will behave somewhere between these two extremes; rotation or overt motion of the target however results in the unambiguous realization of case-2 statistics.

For the unfocused case, with an arbitrary spot size (S) assumed to be $>\sqrt{L/k}$, we have three corresponding realms as shown in Table II. The special case of collimation is given by $S = \alpha_0$.

Finally, we consider physically the covariance characteristics for finite receivers. The result expressed in Eq. (42) implies that the covariance scale for both the coherent or incoherent terms in $C_1(\bar{p})$ will be smeared to the order of the receiver size, with a falloff whose abruptness depends on the point-receiver covariance scales relative to this size. This behavior is obvious: separations less than the receiver size imply overlapping receivers. The variance for a finite receiver will be smoothed in accordance with the effective number of independently scintillating patches in its aperture; the dependence for the incoherent term⁸ is $(D/\sqrt{L/k})^{-7/3}$ in the absence of multiple scattering and a function of (D/ρ_0) for strong scattering; the dependence for the coherent term has not been explicitly obtained but may be expected to be approximately $\left[D/(\alpha_0 \text{ or } \rho_0) \right]^{-2}$.
(smaller)

We point out that, for a receiver large enough to smooth the speckles represented by the coherent term, these speckles become simply a residual noise source and the behavior is otherwise as if the source were incoherent. Referring to Figure 5, the tail of the covariance term then has a more significant effect than the smaller scales.

TABLE I. VARIANCE AND COVARIANCE VS. PARAMETER REALMS
DIFFUSE TARGET/FOCUSED BEAM

$\sqrt{L/k} < \rho_0$		$\sqrt{L/k} > \rho_0$	
$(\sqrt{L/k} < \rho_0 < \alpha_0 - \text{Far Field})$		$(\rho_0 < \sqrt{L/k} < \alpha_0 - \text{Near Field})$	
<div>Case A-1</div> <div>Case A-2</div> $\rho_a \sim \sqrt{L/k}$ $\sigma_{\chi}^2 \sim C_n^2 k^{7/6} L^{11/6}$		$\rho_a \sim \rho_0, L/k\rho_0$ $\sigma_{I_n}^2 = 2e^{4\gamma\sigma_{\chi}^2}$ $\gamma = f(L/k\rho_0, \rho_0) \sim (L/k\rho_0^2)^{-2}$	
<div>$\sqrt{L/k} < \alpha_0 < \rho_0 - \text{Far Field}$</div> <div>Case B-1</div> <div>Case B-2</div> $\rho_a \sim \sqrt{L/k}$ $\sigma_{\chi}^2 \sim C_n^2 k^{7/6} L^{11/6}$		$\rho_a \sim \sqrt{L/k}, \alpha_0$ $\sigma_{I_n}^2 = 2e^{4\gamma\sigma_{\chi}^2}$	
		<div>$(\rho_0 < \alpha_0 < \sqrt{L/k} - \text{Far Field})$</div> $\rho_a \sim \rho_0, L/k\rho_0$ $\sigma_{I_n}^2 = 2e^{4\gamma\sigma_{\chi}^2}$ $\gamma = f(L/k\rho_0, \rho_0) \sim (L/k\rho_0^2)^{-2}$	
<div>$(\alpha_0 < \sqrt{L/k} < \rho_0 - \text{Near Field})$</div> $\rho_a \sim \alpha_0, L/k\alpha_0^2$ $\sigma_{I_n}^2 = 2e^{4\gamma\sigma_{\chi}^2}$ $\gamma \sim (\sqrt{L/k}/\alpha_0)^{-7/3}$		<div>$(\alpha_0 < \rho_0 < \sqrt{L/k} - \text{Near Field})$</div> $\rho_a \sim \alpha_0, L/k\alpha_0^2$ $\sigma_{I_n}^2 = 2e^{4\gamma\sigma_{\chi}^2}$ $\gamma = f(L/k\alpha_0, \rho_0) \sim (L/k\alpha_0\rho_0)^{-2}$	

TABLE II. VARIANCE AND COVARIANCE VS. PARAMETER REALMS
DIFFUSE TARGET/ARBITRARY SPOT ($S > \sqrt{L/k}$)

A	D
B	
	<p>($\rho_0 < L/kS < \sqrt{L/k}$)</p> <p>$\rho_a \sim \rho_0, L/k\rho_0$</p> <p>$\sigma_{I_n}^2 = 2e^{4\gamma\sigma_x^2} - 1$</p> <p>$\gamma = f(L/k\rho_0, \rho_0) \sim (L/k\rho_0^2)^{-2}$</p>
<p>($L/kS < \sqrt{L/k} < \rho_0$)</p> <p>$\rho_a \sim L/kS, S$</p> <p>$\sigma_{I_n}^2 = 2e^{4\gamma\sigma_x^2} - 1$</p> <p>$\gamma \sim (S/\sqrt{L/k})^{-7/3}$</p>	<p>($L/kS < \rho_0 < \sqrt{L/k}$)</p> <p>$\rho_a \sim L/kS, S$</p> <p>$\sigma_{I_n}^2 = 2e^{4\gamma\sigma_x^2} - 1$</p> <p>$\gamma = f(S, \rho_0) \sim (S/\rho_0)^{-2}$</p>
C	F

8. Time-Lagged Covariance

The spatial spectrum of irradiance may be found by taking the Fourier transform of the covariance (Eq. 30). The temporal spectrum requires the time-lagged covariance function, which may be obtained by repeating the procedure of Sec. II-A3 incorporating the time-delay (τ) between irradiance measurements at \bar{p}_1 and \bar{p}_3 respectively. We have the following, corresponding to Eqs. (24, 25, and 27):

$$C_I(\bar{p}_1, \bar{p}_3, \tau) = \langle I(\bar{p}_1) I(\bar{p}_3, \tau) \rangle - \langle I(\bar{p}_1) \rangle \langle I(\bar{p}_3, \tau) \rangle \quad (59)$$

$$B_I(\bar{p}_1, \bar{p}_3, \tau) = (k/2\pi L)^4 \iiint d\bar{\rho}_1 d\bar{\rho}_2 d\bar{\rho}_3 d\bar{\rho}_4 \langle U(\bar{\rho}_1) U^*(\bar{\rho}_2) U(\bar{\rho}_3, \tau) U^*(\bar{\rho}_4, \tau) \rangle \exp \{ ik(R_1 - R_2 + R_3 - R_4) \} H(\bar{r}_1, \bar{\rho}_2, \bar{\rho}_3, \bar{\rho}_4; \bar{p}_1, \bar{p}_3; \tau) \quad (60)$$

$$\begin{aligned} \langle U(\bar{\rho}_1) \cdots U^*(\bar{\rho}_4, \tau) \rangle &= \langle I(\bar{\rho}_1) \rangle \langle I(\bar{\rho}_3, \tau) \rangle \delta(\bar{\rho}_1 - \bar{\rho}_2) \delta(\bar{\rho}_3 - \bar{\rho}_4) (4\pi/k^2)^2 \\ &+ \langle U(\bar{\rho}_1) U^*(\bar{\rho}_1, \tau) \rangle \langle U^*(\bar{\rho}_3) U(\bar{\rho}_3, \tau) \rangle \delta(\bar{\rho}_1 - \bar{\rho}_4) \delta(\bar{\rho}_2 - \bar{\rho}_3) (4\pi/k^2)^2 \end{aligned} \quad (61)$$

where $\langle I(\bar{\rho}_i, \tau) \rangle = \langle I(\bar{\rho}_i) \rangle$

The problem is now complicated, relative to the previous ($\tau = 0$) case, by the time-delay term in the second part of Eq. (61). That is, in order to insert Eq. (61) into (60), we must return to Eq. (3) for $U(\bar{\rho})$. This in turn introduces the time-delayed wave structure function $D_\psi(\bar{r}, \tau)$. The ensuing integrations will again be omitted; the result, which utilizes the results of Appendix B and corresponds to Eq. (30), is

$$C_I(\bar{p}, \tau) = C_{I_1} + C_{I_2} \quad (62)$$

$$C_{I_1} = 2/\pi (k^2/L^6) |U_0|^4 (\alpha_0^2/2)^2 \int_0^\infty r dr e^{-r^2/2\alpha_0^2 - 2(r/\rho_0)^{5/3}}$$

$$\times \int d\bar{\rho} J_0(kr\rho/L) \left[e^{4C_X(\bar{p}, \bar{\rho}, \tau)} - 1 \right] \quad (63a)$$

$$C_{I_2} = (k^2/\pi^2 L^6) |U_0|^4 (\alpha_0^2/2)^2 \int_0^\infty d\bar{r} e^{-r^2/\alpha_0^2 - D_\psi(-\bar{r}, \tau)} \\ \times \int d\bar{\rho} e^{ik \bar{\rho} \cdot \bar{r}/L} H(\bar{\rho}, \bar{p}, \tau) \quad (63b)$$

Work is currently underway on the interpretation of these expressions. In particular the value of $\partial C_I / \partial \tau$ at $\tau = 0$ will give insight into the incremental motion vs. evolution of the scintillation pattern.

II-B. Complex Targets and Sources

The preceding considerations were based on the assumption of a perfectly diffuse target. In order to predict the effects of real targets, such features as glints, boundaries, and phase correlation areas (specular components) must be included. In addition, the imperfect temporal and spatial characteristics of real lasers may have an influence and should be understood.

These topics are currently under study, and introductory considerations will be briefly presented in this section. Ultimately, it will be fruitful to extend this work to more general target models and scenarios, including particular wavelengths of interest, moving target/transceiver configurations, and slant paths; and to deal directly with turbulence- and target-driven effects on coherent adaptive transmitter systems.

1. Target Truncation

The simplest example of a nonideal target is a diffuse surface with boundaries. To the extent that the boundaries (which might represent sub-

features of a more complex target) appreciably truncate the target-spot, there will be a component of high spatial frequencies at the target and low frequencies at the receiver. I.e., there will be larger speckles at the receiver, which may represent a significant noise source in a finite aperture.

We again treat a focused beam, where the extension to a more general focal condition is straightforward as in the preceding developments. We assume a round target of radius (a). Referring to Eqs. (8), (19) we have for the mean receiver irradiance:

$$\langle I(\bar{p}) \rangle = \frac{k^2 U_0^2 \alpha_0^2}{L^4} \int_0^a \rho d\rho \int_0^\infty r dr J_0(k \rho r/L) e^{-r^2/4\alpha_0^2 - (r/\rho_0)^{5/3}} \quad (64)$$

For a more general target shape, (S), we can write

$$\langle I(\bar{p}) \rangle = \frac{k^2 U_0^2 \alpha_0^2}{L^4} \int_0^\infty r w(r) e^{-r^2/4\alpha_0^2 - (r/\rho_0)^{5/3}} dr \quad (65)$$

$$\text{where } w(r) \equiv 1/2\pi \int_S d\bar{\rho} J_0(k \rho r/L). \quad (66)$$

In the present case,

$$w(r) \approx (a^2/2) \frac{2J_1(kar/L)}{kar/L} \quad (67)$$

Similarly, we write the covariance from Eq. (29) with appropriate limits on $\bar{\rho}_1, \bar{\rho}_3$, and let $\bar{\rho}_1 - \bar{\rho}_3 \equiv \bar{\rho}$, $\bar{\rho}_1 + \bar{\rho}_3 \equiv 2\bar{R}$:

$$C_I(\bar{p}) = \frac{1}{\pi^2 L^4} \iint d\bar{\rho} d\bar{R} \langle I(\bar{R} + \bar{\rho}/2) \rangle \langle I(\bar{R} - \bar{\rho}/2) \rangle \\ w_0(\bar{R} + \bar{\rho}/2) w_0(\bar{R} - \bar{\rho}/2) \left\{ \left(e^{4C_X(\bar{p}, \bar{\rho})} - 1 \right) + e^{ik \bar{p} \cdot \bar{\rho}/L} H(\bar{p}, \bar{\rho}) \right\} \quad (68)$$

where $w_0(\bar{x}) = 1$ for $|\bar{x}| \leq a$ and zero otherwise, and

$$\langle I(\bar{R} \pm \bar{\rho}/2) \rangle = (k/L)^2 U_0^2 \alpha_0^2 / 2 \int_0^\infty r J_0(k r |\bar{R} \pm \bar{\rho}/2|/L) \\ e^{-r^2/4\alpha_0^2 - (r/\rho_0)^{5/3}} dr \quad (69)$$

The result is somewhat more complex than that of Eq. (30) for an infinite target. A full interpretation and numerical evaluation remains to be completed. However, the physical implications can be generally deduced. Let us assume that (a) is much smaller than the spot size determined by α_0 :

Coherent term: the speckles scale arising from the target will be $\sim L/ka \gg \alpha_0$. Phase perturbations will cause a normalized variance of unity; amplitude perturbations may have a stronger additional effect than in the infinite-target case, since the total power hitting the target may now vary.

Incoherent term: The limited size of the target may reduce or eliminate spot-size smoothing of the receiver scintillations, which will be further enhanced by variations in the total power hitting the target.

We note here a very interesting prediction that may be subjected to numerical and experimental verification, and which could have profound effects on optical system operation. Suppose that the target (or some feature on the target) is smaller than the scales of interest, i.e., $\alpha < \rho_0, \sqrt{L/k}$. We may then utilize δ -functions on $\bar{\rho}, \bar{R}$ in Eqs. (68,69) and find that the variance is given by

$$\sigma_{I_n}^2 = \left(e^{4\sigma_\chi^2} - 1 \right) + \left(e^{4\alpha_\chi^2} \right), \quad (70)$$

where we have again deliberately separated the contributions from the incoherent and coherent terms respectively. This expression is consistent with Eq. (55) with $\gamma=1$, as expected.

We now note that for a small source in strong turbulence ($\rho_0 < \sqrt{L/k}$), the saturated variance for the incoherent term is unity.¹¹ This implies that $e^{4\sigma_\chi^2} = 2$. Hence under the present condition, wherein the effective target spot is constrained to be small through target truncation, strong turbulence may result in a total normalized variance of 3, which is indeed substantial. This effectively comes about through a combination of varying phase perturbations (speckles) and saturated amplitude scintillations from the target-spot to the receiver. (It is of course assumed that the diffuse target has sufficient extent to create speckles, which are modulated by the turbulence and/or target motion.) The variance of 3 can in fact be simply related to the fol-

11. R. Fante, "Electromagnetic Beam Propagation in Turbulent Media", Proc. IEEE, 63, 1669, Dec. 1975.

lowing:

Let random independent processes (x,y) have normalized variances of unity.

Let $z \equiv xy$

Then

$$\frac{\sigma_z^2}{\langle z \rangle^2} = \frac{\langle x^2 y^2 \rangle}{\langle xy \rangle^2} - 1 = \frac{\langle x^2 \rangle \langle y^2 \rangle}{\langle x \rangle^2 \langle y \rangle^2} - 1$$

3

If we identify (x,y) with (saturated) amplitude and phase-induced irradiance fluctuations respectively, we derive the expected total variance of 3.

Further insight can be gained by considering the case of a one-way path from a finite, diffuse source. We assume that this source has a diameter D and uniform irradiance I_0 . From Eq. (29) and the overlap integral such as used in Sec. II-A5, we immediately write the covariance as

$$C_I(\bar{p}) = \frac{I_0^2}{4\pi} (D/L)^4 \int_0^1 x dx \int_0^{2\pi} d\theta M(x) \left\{ \left(e^{4C_X(Dx, \bar{p})} - 1 \right) + e^{ik(D/L) \bar{p} \cdot \bar{x}} H(Dx, \bar{p}) \right\} \quad (71)$$

where $\bar{x} \equiv \bar{p}/D$, θ is the angle between \bar{p} and \bar{p} , and

$$M(x) = 2/\pi \left[\cos^{-1} x - x\sqrt{1-x^2} \right] \quad (72)$$

Since $\langle I(\bar{p}) \rangle = I_0 \frac{\pi D^2}{4} \times \frac{1}{\pi L^2}$ from Lambert's Law, the normalized variance is

$$\sigma_{I_N}^2 = 8 \int_0^1 x M(x) \left[2e^{4C_X(Dx)} - 1 \right] dx \quad (73)$$

For D less than the characteristic scale of C_x , Eq. (73) reduces to Eq. (70).

It is at first perhaps curious that the same result for the variance was obtained for both the small target and the small diffuse-source cases. This suggests that any fluctuation (scintillation) of the total energy on the target is not taken into account in Eq. (68). This is indeed the case; as discussed in conjunction with Eq. (27), the assumption of gaussian field statistics after reflection from the target implicitly drops such fluctuations. The small-target, strong-scintillation situation represents a practical case where this assumption may not be valid and a more complete treatment, including irradiance statistics on the target, should be used. This in turn implies that the receiver variance may be greater even than 3.

2. Glints

An analysis of the mean irradiance pattern at the receiver for an arbitrary number of glints on the diffuse target was given in the preceding report. We have subsequently derived the mutual coherence function and covariance under the assumption of joint gaussian field statistics. The limitations of this assumption have been pointed out in the discussions of this report, and an extension of the theory is underway.

3. Nonideal Sources

The temporal and spatial coherence characteristics of real lasers, especially in the case of many high power, infrared units of interest, cannot be neglected. The nonzero spectral width covered by one or a series of laser lines (transitions) may result in sharply reduced speckle contrast in the coherent term of the variance, and possibly even spectral smoothing of the incoherent term in the presence of strong turbulence. These effects will be observed if, as is the case in the initial experiments described in Section IV, the spectral width leads to a "coherence length" which is less than the path-length-differences involved in the optical system-target-atmosphere geometry. In addition, transverse mode structure can increase the focused target-spot-size and therefore affect the received field.

The effects of finite spectral width on speckles in the absence of

turbulence have been heavily researched in the past few years.¹²⁻¹⁵ The extension of the current theory to include both temporal and spatial coherence effects in turbulence is currently underway.

A heuristic approach is suggested as follows. We separate the coherent and incoherent parts of the variance (Eq. 55):

$$\sigma_n^2 = \gamma_1 e^{4\gamma_2 \sigma_X^2} + (e^{4\gamma_2 \sigma_X^2} - 1) \quad (74)$$

where

γ_1 = reduction in speckle contrast owing to source spectral width

γ_2 = source (target-spot) smoothing

While it is recognized that γ_1 will vary with the details of transmitter-target-receiver geometry, including spot-size, this simple approach is shown to give reasonable qualitative agreement with experiments in Section IV.

III. Numerical Evaluations

The results of Section II for such statistical descriptors as the covariance of irradiance are generally in the form of multiple-dimensioned integrals. While amenable to meaningful physical interpretation, accurate quantitative predictions from these expressions requires numerical evaluation. The purpose of this section is to present a simplifying technique which has made the problem tractable by greatly reducing the time required on a computer of reasonable capacity and speed. Preliminary results are given and compared with experiments in Section IV.

-
12. J. C. Dainty, "Some Statistical Properties of Random Speckle Patterns in Coherent and Partially Coherent Illumination", *Optica Acta* 17, 761, 1970.
 13. G. Parry, "Some Effects of Temporal Coherence on the First Order Statistics of Speckle", *Optica Acta* 21, 763, 1974.
 14. H. M. Pederson, "On the Contrast of Polychromatic Speckle Patterns and its Dependence on Surface Roughness", *Optica Acta* 22, 15, 1975.
 15. H. M. Pederson, "Second-Order Statistics of Light Diffracted from Gaussian, Rough Surfaces with Applications to the Roughness Dependence of Speckles", *Optica Acta* 22, 523, 1975.

III-A. Basic Technique

The five-fold integrations required in expressions such as (30) initially appear rather formidable. The use of Monte Carlo techniques is hampered by the form of the integrand and the interdependency of the integration limits. An analytic technique, however, permits accurate evaluation, as follows.

The form of the integrands in Eq. (30) is

$$C_{I_1}(\bar{p}) \sim \iiint d\theta dr d\rho \quad r\rho \left(e^{4C_X(\bar{\rho}, \bar{p})} - 1 \right) J_0(kr\rho/L) f_1(r) \quad (75)$$

$$C_{I_2}(\bar{p}) \sim \iiint d\theta dr d\rho \quad r\rho J_0(kr\rho/L) f_1(r) f_2(\bar{\rho}, \bar{p}) \quad (76)$$

$$\text{where } f_1(r) = \exp \left\{ -r^2 \left(\frac{1}{2\alpha_0^2} - \frac{k^2}{2L^2} \right) - \alpha_0^2 (1 - L/F)^2 \right\} - 2(r/\rho_0)^{5/3} \quad (77)$$

for a general focus, and

$$f_2(\bar{\rho}, \bar{p}) = e^{ik \cdot \bar{p} \cdot \bar{\rho} / L} H(\bar{\rho}, \bar{p}). \quad (78)$$

We note that θ is the angle between \bar{p} and $\bar{\rho}$.

Each of the integrands contains the term

$$r J_0(kr\rho/L) f_1(r)$$

Our approach is to expand $f_1(r)$ in a Fourier-Bessel series and then utilize

$$\int_0^\infty r J_0(\alpha r) J_0(\beta r) dr = 2\delta(\alpha - \beta) / (\alpha + \beta) \quad (79)$$

to simplify the integration. The expansion is given by

$$f_1(r) = \sum_m b_m J_0(\rho_m r/A) \quad (80)$$

where

$$b_m = \frac{2}{A^2 J_1^2(\rho_m)} \int_0^A x f_1(x) J_0(\rho_m x/A) dx \quad (81)$$

and

$$J_0(\rho_m) \equiv 0 \quad (82)$$

The utility of the expansion stems from the fact that $f_1(r)$ becomes negligible for some value (A) of r that is readily calculated and not dependent on the other integration limits, and its shape is such that it can be represented by only a few (e.g. 6) terms in the series.

The covariance may now be rewritten

$$C_I(\bar{p}) \sim \sum_m b_m \int d\theta \left[e^{4C_X(L\rho_m/k A, p, \theta)} - 1 + f_2(L\rho_m/k A, p, \theta) \right] \quad (83)$$

The normalized variance is simply

$$\sigma_{I_n}^2 = \sum_m b_m \left[2e^{4C_X(L\rho_m/k A)} - 1 \right] \quad (84)$$

III-B. Variance of Irradiance

The log amplitude covariance functions (C_X) now comprise the limiting factor in generating numbers from the theory. In the case of the variance, where $\bar{p} = 0$, the unsaturated covariance can be represented by a six-term

series.¹⁶ The strongly saturated case can be handled by Eq. (A5), which is readily evaluated using standard numerical integration techniques. The transition region between the unsaturated and saturated conditions can in principle be handled using a general expression in Ref. 17; however, this function is highly complicated.

The numerical evaluations of the variance are given in Section IV, Figure 7.

III-C. Cavariance of Irradiance

The unsaturated two-source log amplitude covariance required in Eq. (83) has not yet proven amenable to simple series expansion representation. We are continuing to examine this problem; in the meantime, a two-fold gaussian quadrature technique is being used, which is somewhat time consuming on the computer but which is resulting in numbers that agree well with experiment (Figure 12, Section IV).

The saturated case is further complicated by the fact that a two-source covariance function in multiple scattering has not yet been derived by analytical investigators.¹⁸

IV. Experimental Results

IV-A. Introduction

An experimental program to verify the theory was described in Ref. 1 and has been fully underway for several months. The measurements are made with an argon laser at 4880\AA over path lengths up to 1 km. The facility and instrumentation are as described previously, with certain additions noted below.

In the course of these experiments, three difficulties have been uncovered. First, it has been found that the argon laser has sufficient doppler-broadened spectral linewidth (~ 10 GHz) to significantly reduce the variance of irradiance observed from a diffuse target (speckles) in the absence of turbulence. In order to alleviate this difficulty, the laser was

16. D. L. Fried, "Propagation of a Spherical Wave in a Turbulent Medium", J. Opt. Soc. Am. 57, 175, February 1967.
17. S. F. Clifford and H. T. Yura, "Equivalence of Two Theories of Strong Optical Scintillation", JOSA 64, 1641, December 1974.
18. H. T. Yura, Aerospace Corp., private communication.

substantially modified to include the insertion of a temperature stabilized, intra-cavity etalon which resulted in single-axial-mode operation and elimination of this effect.

Second, it was found that in the case of the very small covariance scales that can result under conditions of strong turbulence and/or a large target spot, the receiver apertures must be impractically small in order to resolve the covariance curve and measure the proper (unsmoothed) variance. Similarly, the resolution of the receiver separation must be very high. In order to make such small apertures and highly resolved separations practical, two telescopes were fabricated for insertion in front of the apertures. This resulted in the characteristics shown in Table III.

TABLE III. RECEIVER PARAMETERS VS. TELESCOPE ATTACHMENT

Magnification	Effective Receiver Aperture (mm)	Minimum Separation (mm)	Relative Detector Energy
1 (no telescope)	2.0	4.5	1.0
1.7	1.18	2.65	0.35
3.1	0.38	1.45	0.10

The third difficulty is more fundamental. It is of course desirable to operate in all six parameter realms as outlined in Table I. However, as described in the preceding paragraph, in the case of a large target-spot, the receiver must be quite small and will in principle receive a small fraction of the transmitted optical power. In general, if the target spot-size is D , the fraction of the power reflected into a Lambertian hemisphere which is intercepted by a receiver of size L/kD is of order

$$\frac{L^2/k^2D^2}{L^2} \sim (kD)^{-2} \sim (\text{target spot-size in wavelengths})^{-2}$$

This is a small number and independent of pathlength. An equivalent viewpoint directly relatable to Table I is that a small transmitter of size (α_0) will result in speckles of the same size, with a fractional receiver energy of order $(\alpha_0/L)^2$; in order to reach parameter realms C, F, and E, α_0 will be constrained to be smaller than $\sqrt{L/k}$ and hence $(\alpha_0/L)^2 < \lambda/L$. In the event that multiple scattering results in atmospheric speckles (ρ_0) smaller yet, the problem is compounded further.

It is felt that the current experimental program is sufficiently comprehensive to verify the theory presented in Section II. Certain parameter realms would be more amenable to investigation with high-energy pulsed lasers; however, the realms of most interest, in which the energy is concentrated on the target (focused) to whatever degree the atmosphere permits in the absence of an adaptive transmitter, are readily handled with the cw facility.

In addition to completing the experiments described here, future work will involve more complex targets including multiple glints; and may include wavelength scaling (e.g. 3.8 μ) and relative translation between the target and receiver.

IV-B. Variance Measurements

Variance measurements prior to the use of an etalon in the laser are shown in Figure 6. The heuristic curve of Eq. (74) is also shown, with γ_1 determined from small- σ_x measurements as being 0.33. The value of γ_2 is taken as unity for simplicity; it will begin to drop from that value at the largest values of the abscissa, where ρ_0 approaches the transmitter size. Although this approach, and especially the use of a fixed value of γ_1 , are somewhat crude, the general behavior is properly predicted.

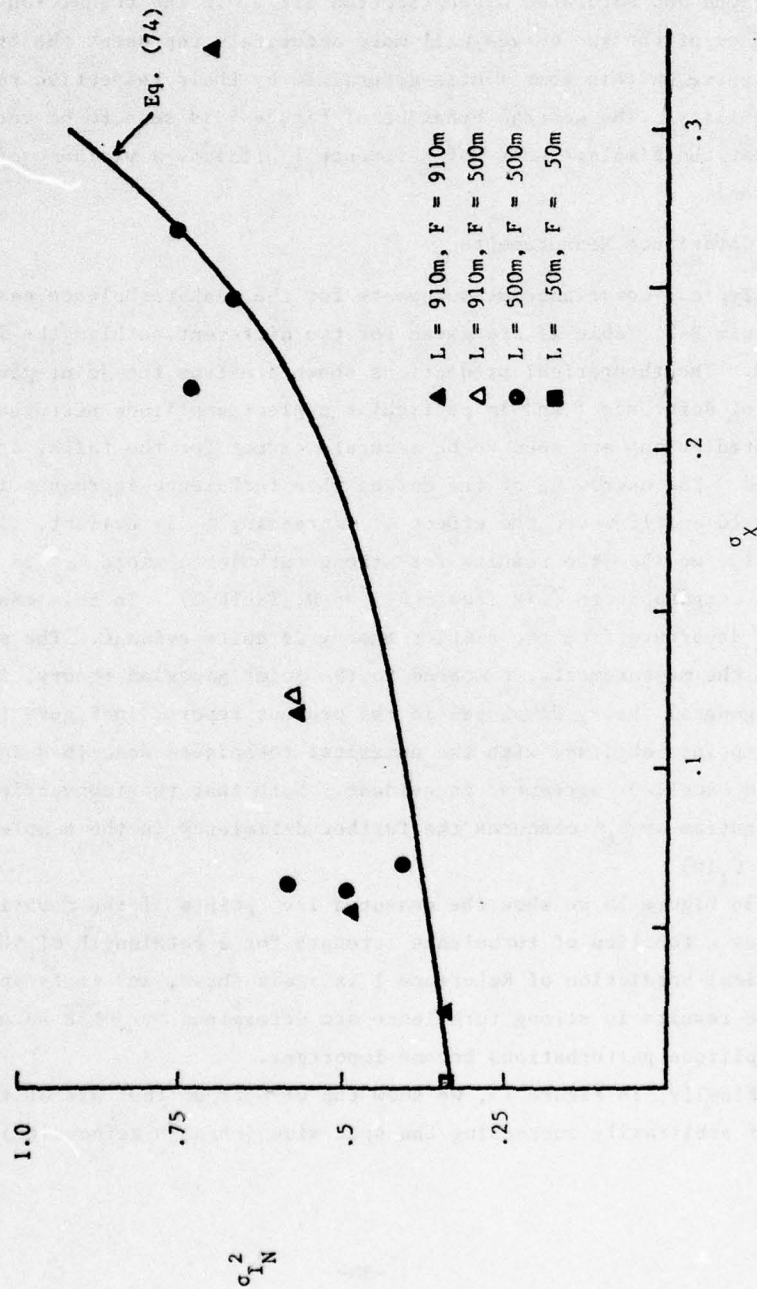


Figure 6. Normalized Variance for a Focused Transmitter vs. Log Amplitude Standard Deviation for a Point Source (prior to etalon).

Values obtained over a 500m path with the insertion of an intracavity etalon are shown in Figure 7, along with the numerical predictions for the unsaturated and saturated cases (Section III). In the transition region, the higher of the two curves will more accurately represent the true composite curve, within some limits determined by their respective ranges of applicability. The general behavior of Figure 4 is seen to be verified. Note that the simpler theory of Reference 1 predicts a variance of unity in all cases.

IV-C. Covariance Measurements

Typical covariance measurements for the weak-turbulence case (parameter realm B-2, Table I) are given for two different pathlengths in Figures 8 and 9. The theoretical predictions shown are from the joint-gaussian theory of Reference 1 and in particular neglect amplitude perturbations. These predictions are seen to be accurate except for the tails, as may be expected. The narrowing of the curves when turbulence increases is shown in Figures 10 and 11 where the effect of decreasing ρ_0 is evident. In Figures 12 and 13, we show the results for strong turbulence where ρ_0 is less than α_0 and comparable to $\sqrt{L/k}$ (realm A-2 or D, Table I). In this case, the serious departure from the simpler theory is quite evident. The substantial tail on the measurements, compared to the joint gaussian theory, is explained by the general theory developed in the present report; in Figure 12 we show several points obtained with the numerical techniques described in Section III, and excellent agreement is evident. Note that the (conventional) normalization by c_1^2 obscures the further deficiency in the simpler theory, i.e. at $C_1(0)$.

In Figure 14 we show the measured $1/e^2$ points of the covariance curves as a function of turbulence strength for a pathlength of 500m. The theoretical prediction of Reference 1 is again shown, and it is apparent that the results in strong turbulence are determined by $\sqrt{L/k}$ as expected when amplitude perturbations become important.

Finally, in Figure 15, we show the effects on the tail of the covariance of arbitrarily increasing the spot size (through defocusing). The

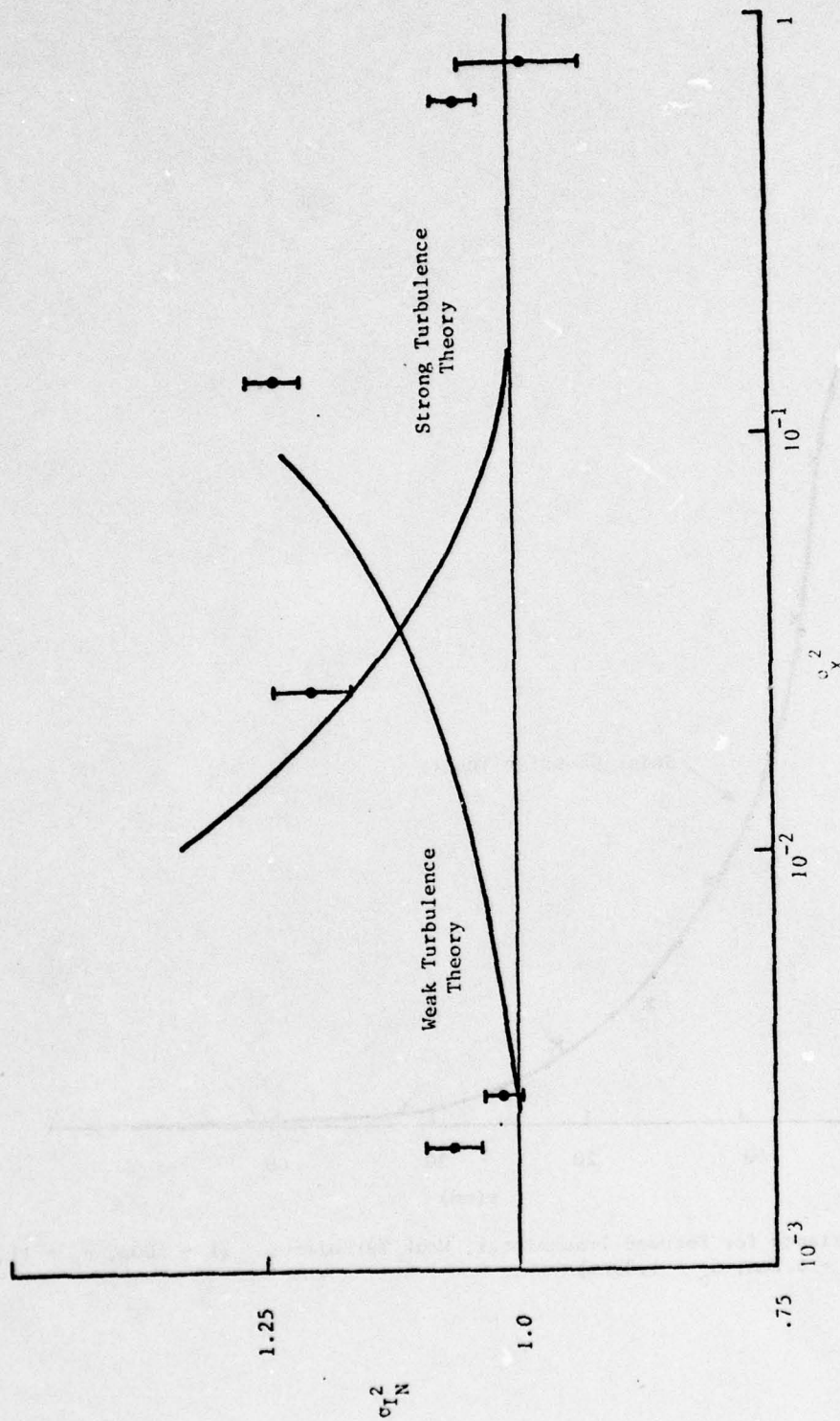


Figure 7. Normalized Variance for a Focused Transmitter vs. Log Amplitude Variance for Point Source. (Etalon Inserted) $L = 500m$.

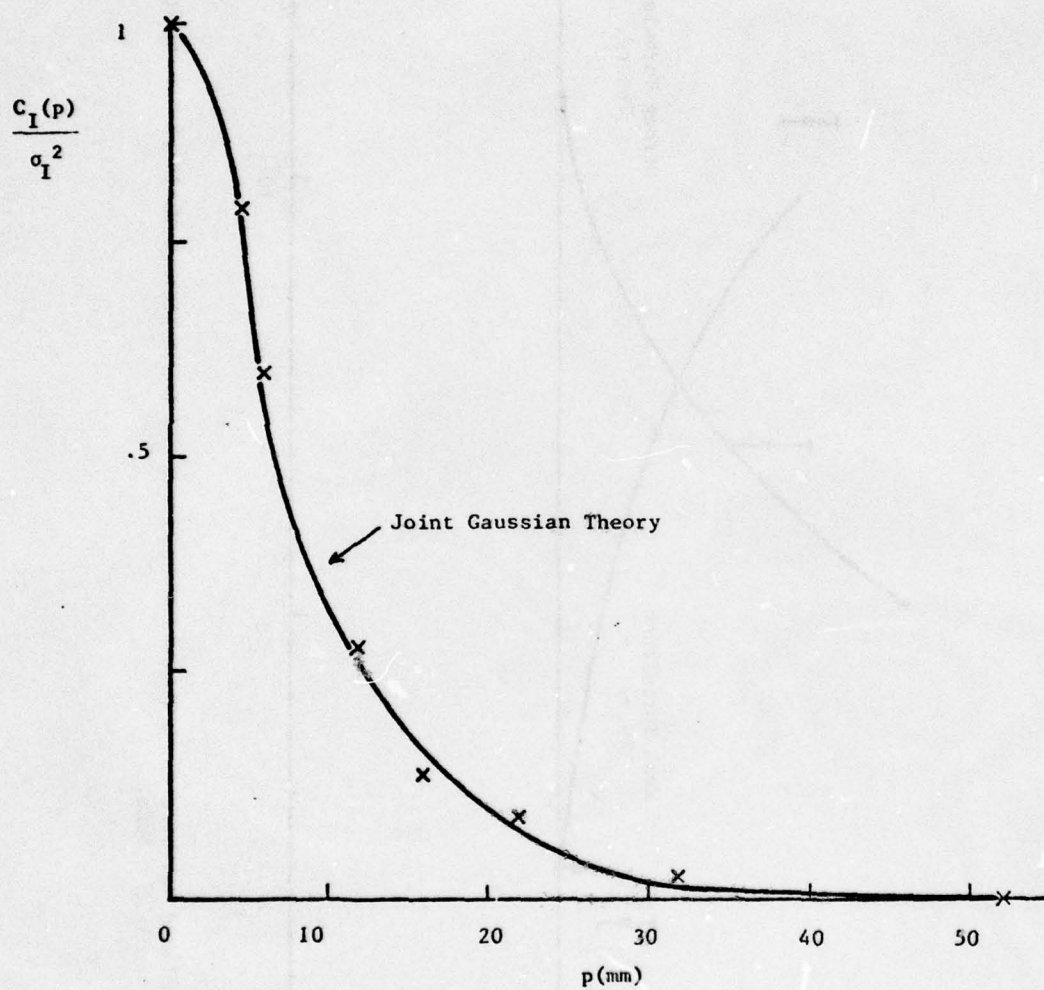


Figure 8. Covariance for Focused Transmitter, Weak Turbulence. ($L = 500\text{m}$, $\rho_0 = 11.5\text{ cm}$, $\sqrt{L/k} = 6.2\text{mm}$, $\alpha_0 = 1.35\text{cm}$)

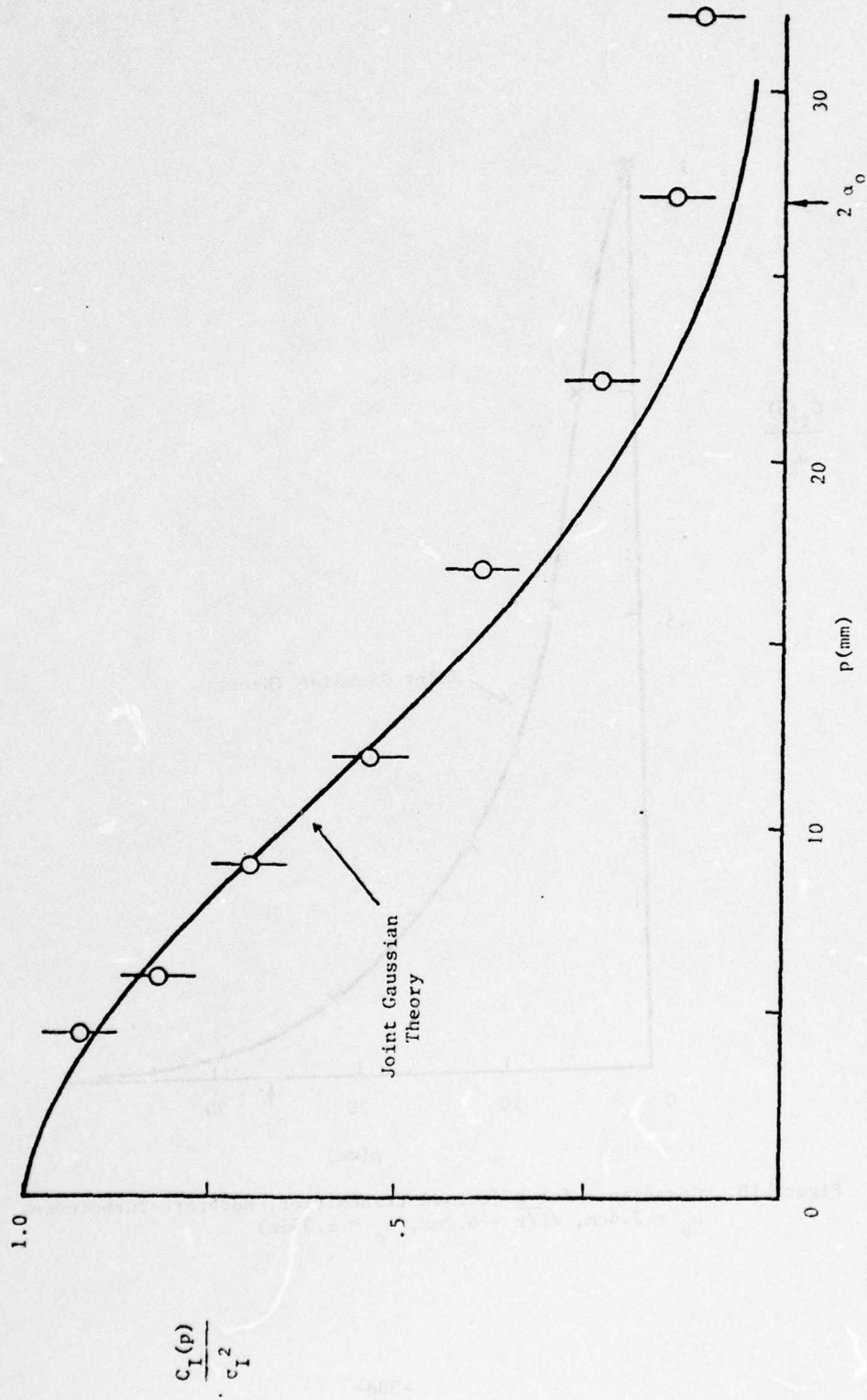


Figure 9. Covariance for Focused Transmitter, Weak Turbulence. ($L = 910m$, $\rho_0 = 7.1$ cm, $\sqrt{L/k} = 8.4mm$, $\alpha_0 = 1.35cm$).

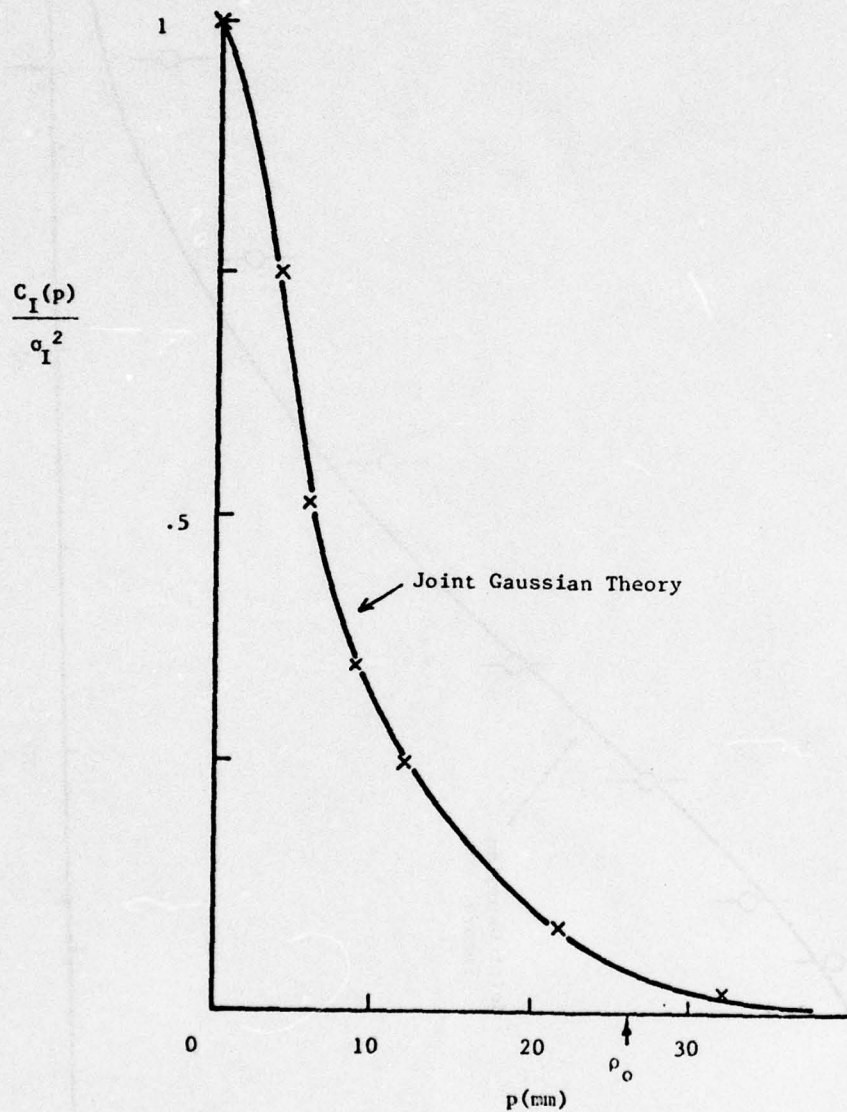


Figure 10. Covariance for a focused transmitter, Moderate Turbulence. ($L = 500\text{m}$, $\rho_0 = 2.6\text{cm}$, $\sqrt{L/k} = 6.2\text{mm}$, $\alpha_0 = 1.35\text{cm}$)

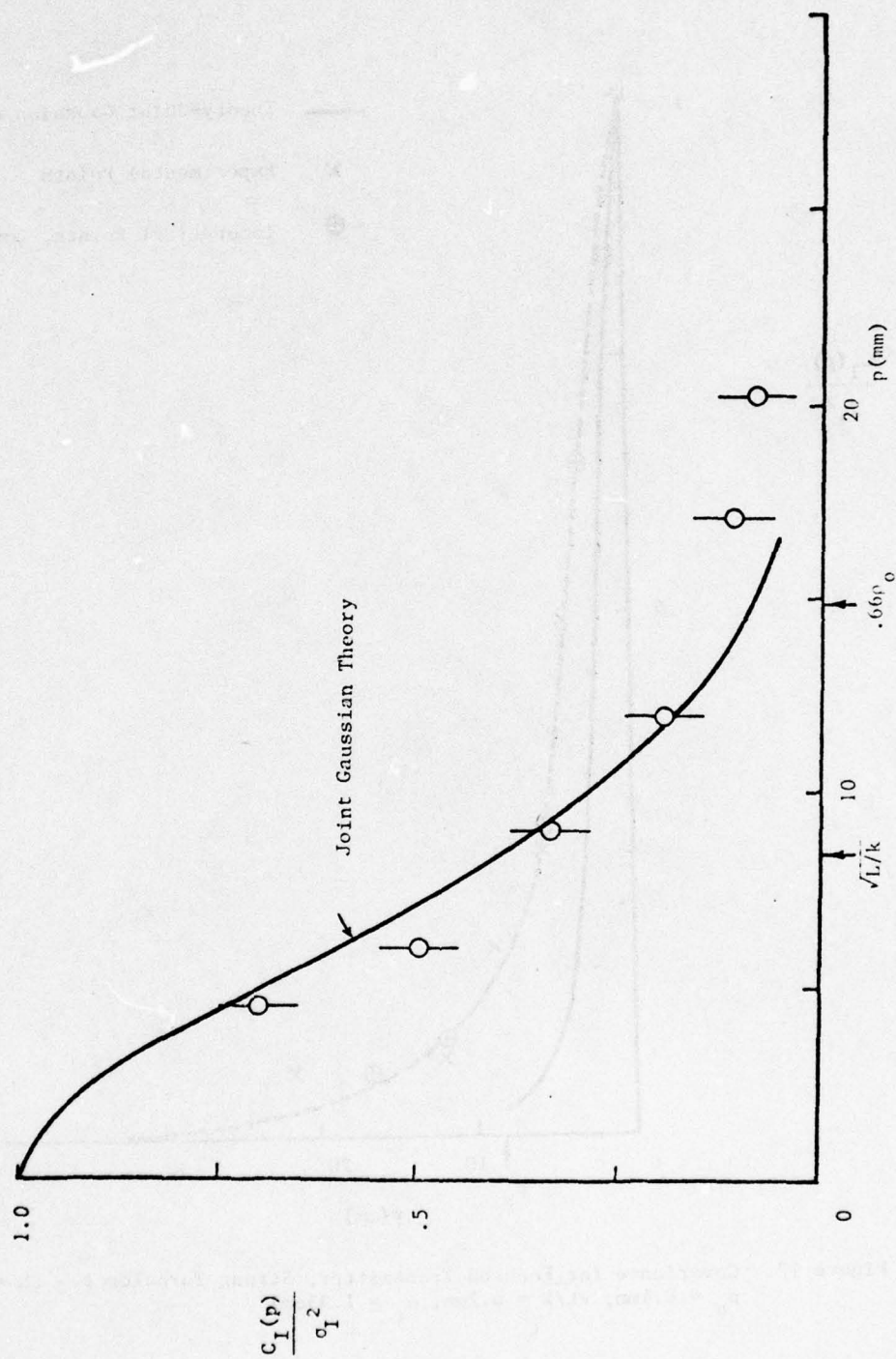


Figure 11. Covariance for Focused Transmitter, Moderate Turbulence. ($L = 910\text{m}$, $\sigma_0 = 2.3\text{cm}$, $\sqrt{L}/k = 8.4\text{mm}$, $\alpha_0 = 1.3\text{e-6}$)

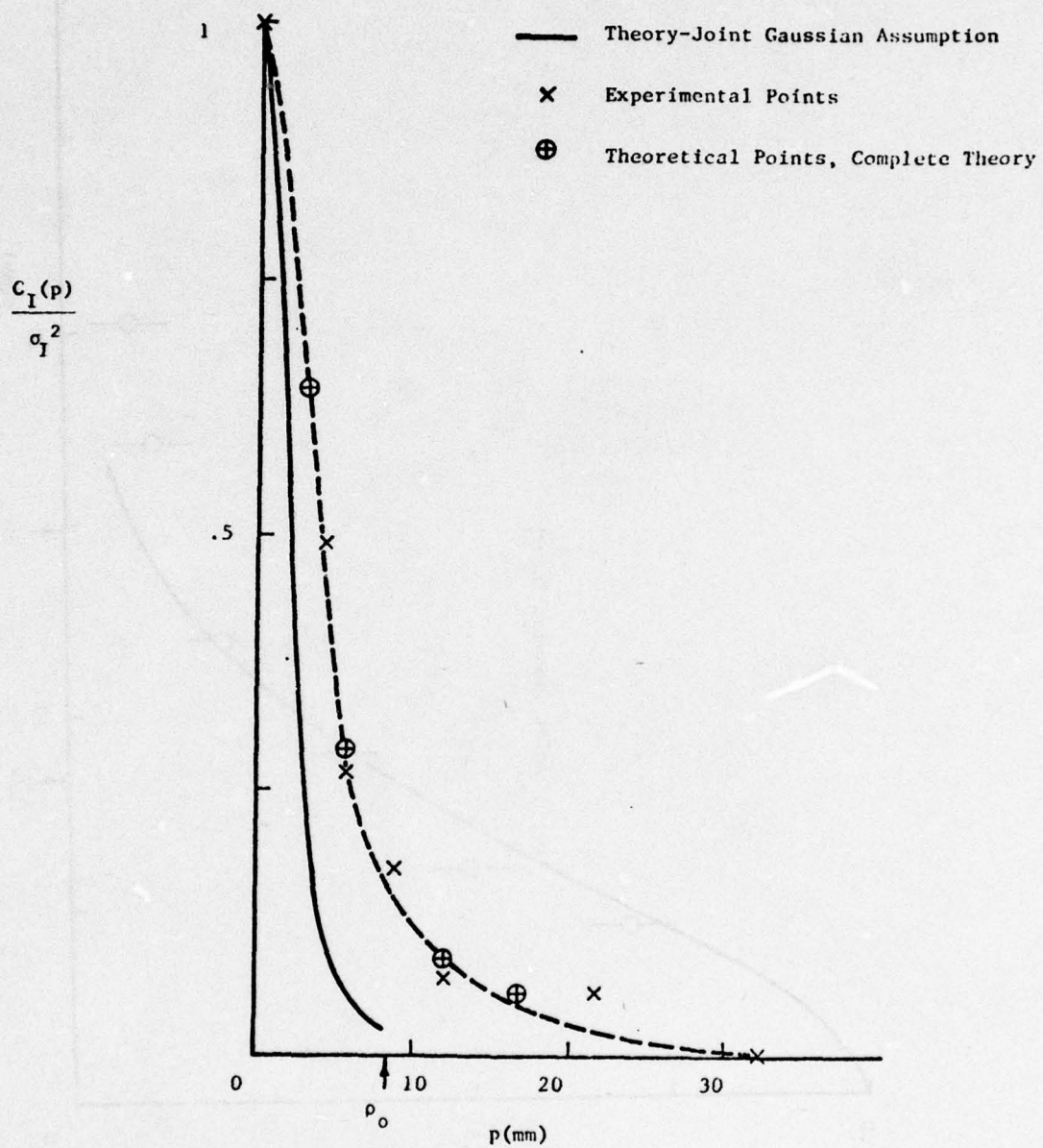


Figure 12. Covariance for Focused Transmitter, Strong Turbulence. ($l = 500\text{m}$, $\rho_0 = 8.4\text{mm}$, $\sqrt{L/k} = 6.2\text{mm}$, $\alpha_0 = 1.35\text{cm}$)

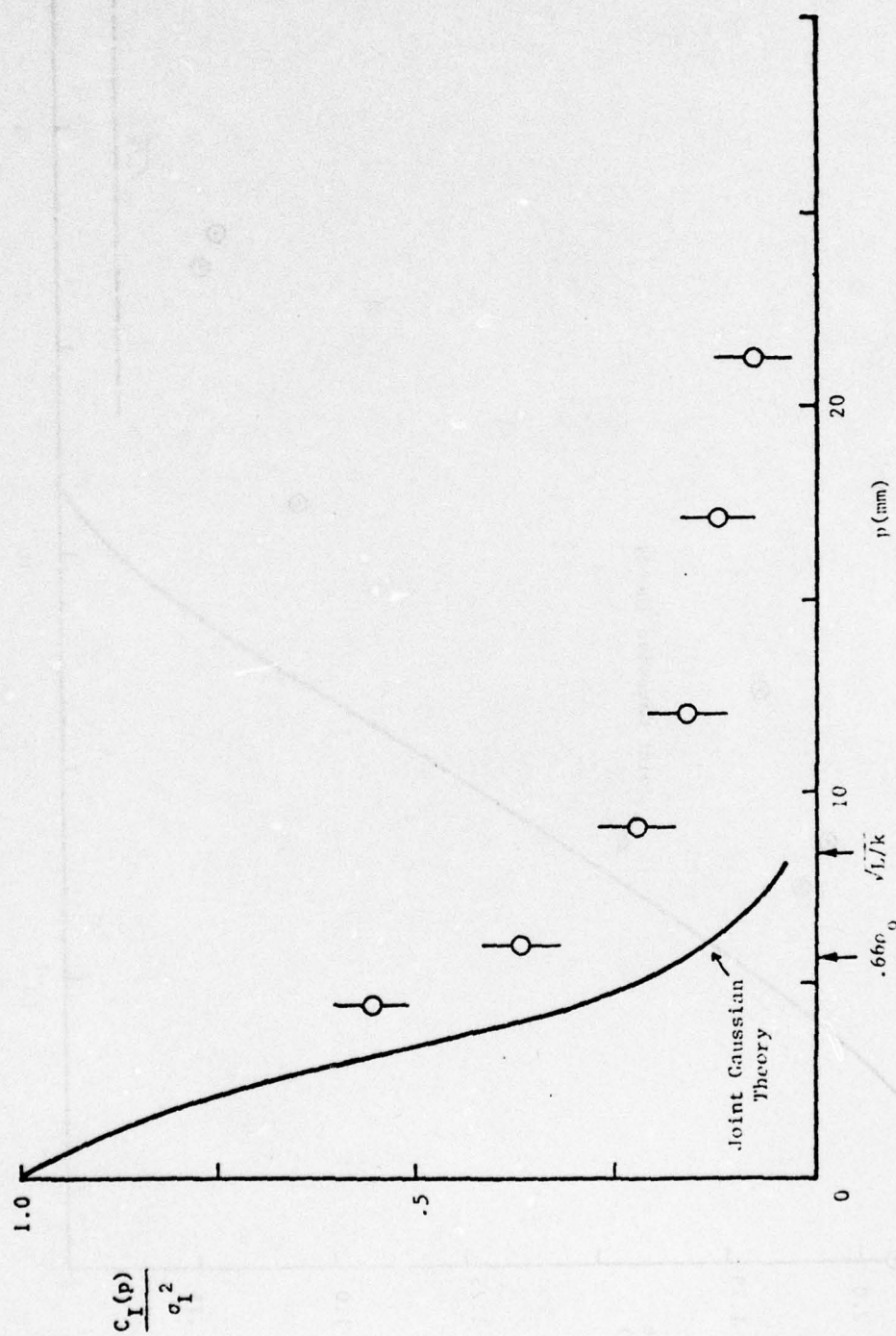


Figure 13. Covariance for Focused Transmitter, Strong Turbulence. ($L \approx 910m$, $\rho_0 \approx 9.6mm$, $\sqrt{L}/k \approx 8.4mm$, $\alpha_0 = 1.35cm$).

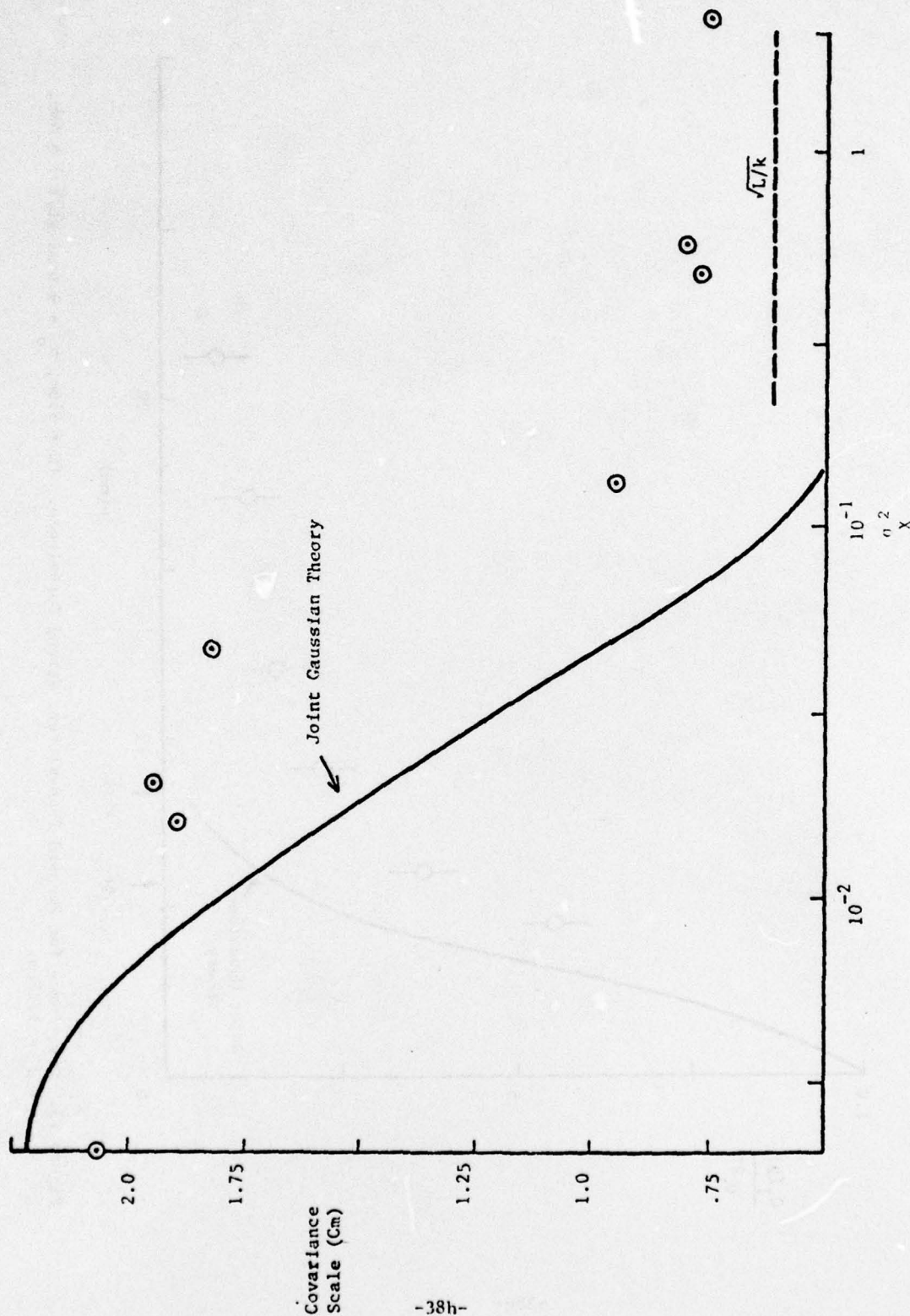


Figure 14. Covariance Scales vs. σ_X^2 for Focused Transmitter ($L = 500m$).

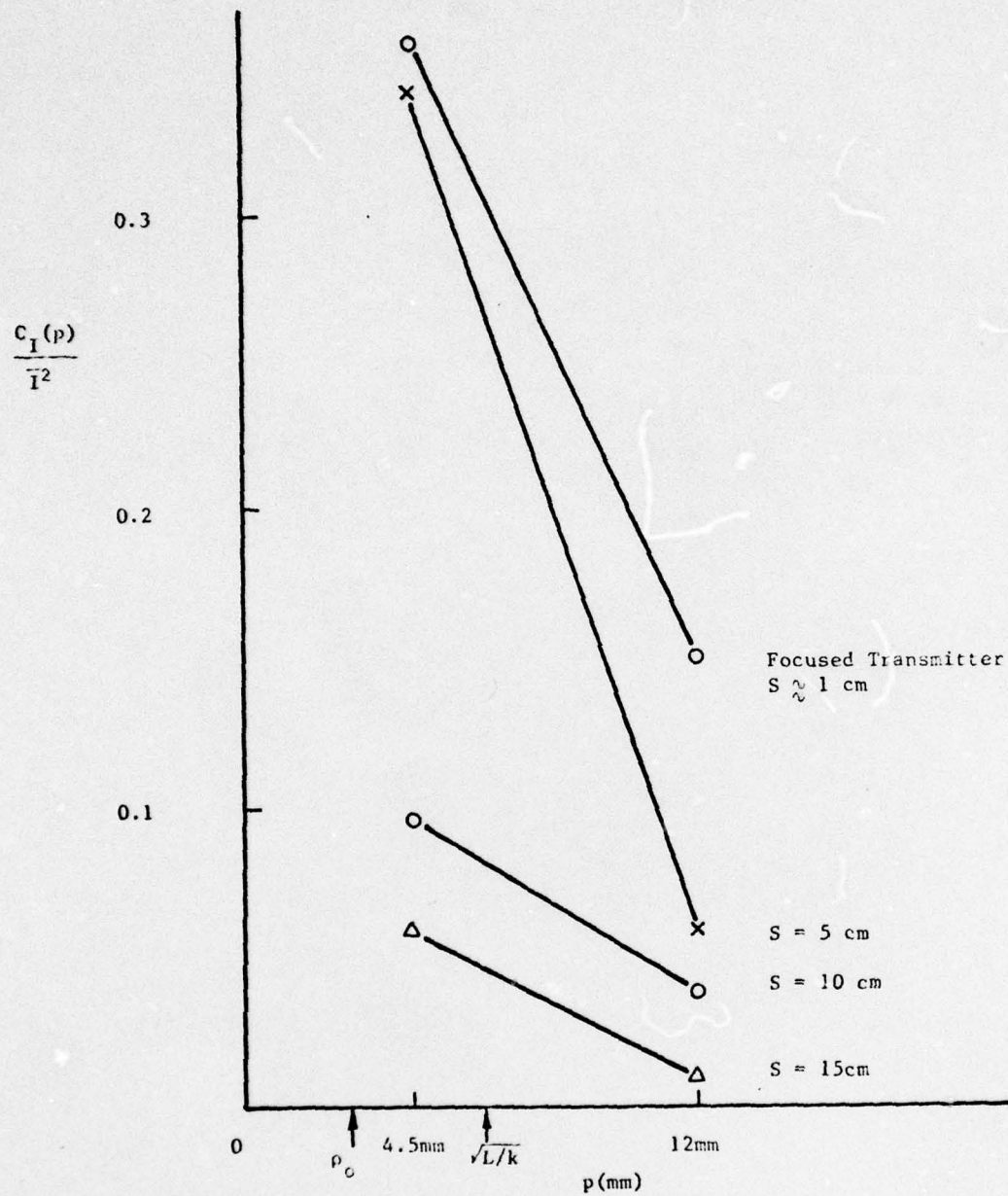


Figure 15. Tail of Covariance Function vs. Increasing Target Spot Size.

reduction of the slope and level of the covariance, through spot-size smoothing, is evident; at sufficiently large separations, larger spots may be expected to give greater residual covariances than smaller spots.

IV-D. Other Properties of the Irradiance

As discussed in Section II, we expect the probability distribution of irradiance to be substantially exponential in the case of weak turbulence. A typical result is shown in Figure 16, along with a plot of an exponential distribution having the measured mean value. The experimental normalized variance is 1.02, while unity is consistent with the exponential distribution.

In stronger turbulence, we expect a combination of exponential and log normal statistics. A typical experimental result, which is in qualitative agreement with this expectation, is shown in Figure 17. Note that the values at small irradiance may be contaminated by system noise. The experimental normalized variance for this case is 1.2.

The existing and ongoing data will also be used for the computation of temporal power spectra and time-lagged covariance functions.

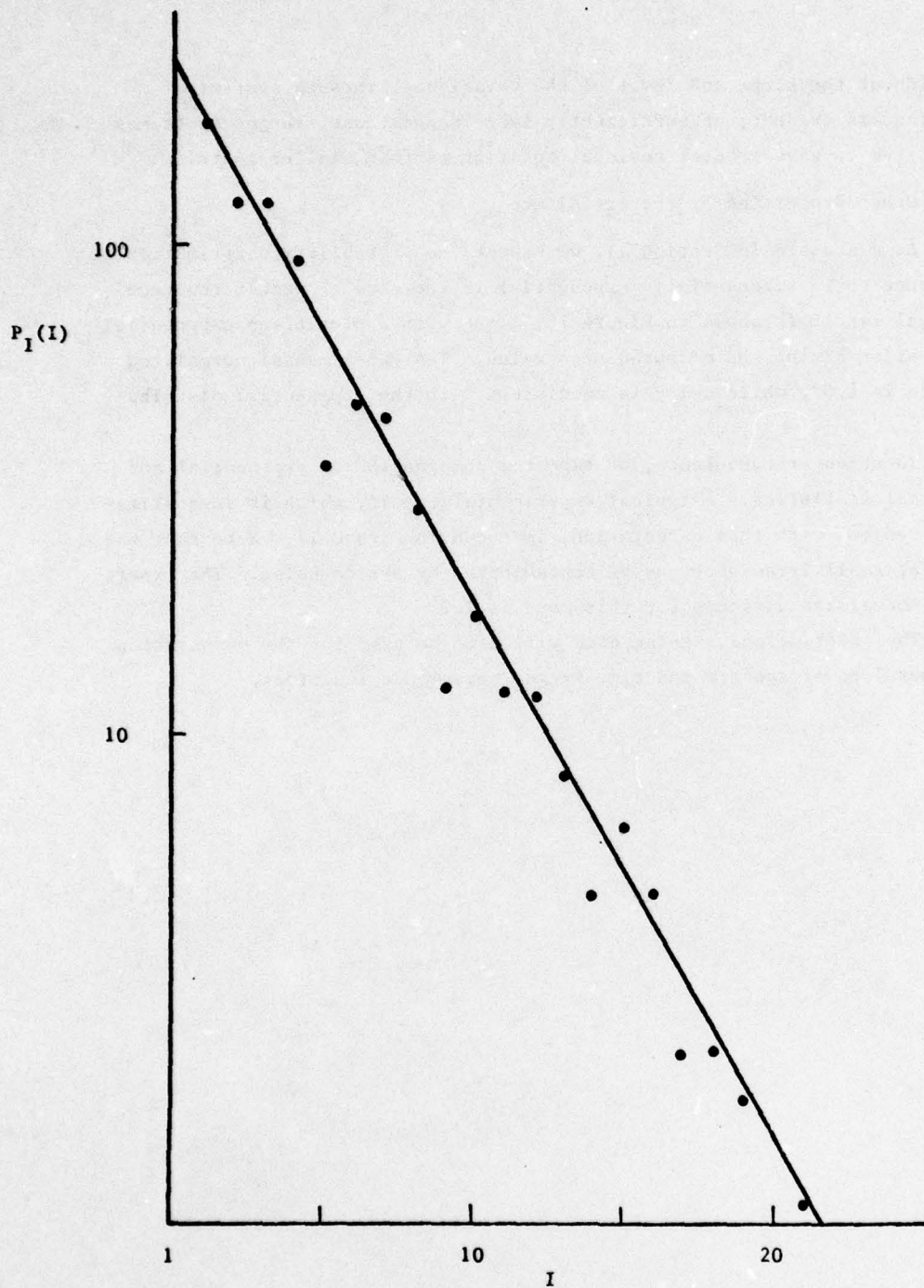


Figure 16. Measured Probability Distribution of Irradiance, Weak Turbulence ($L = 500\text{m}$, $\sigma_{I_N}^2 = 1.02$).

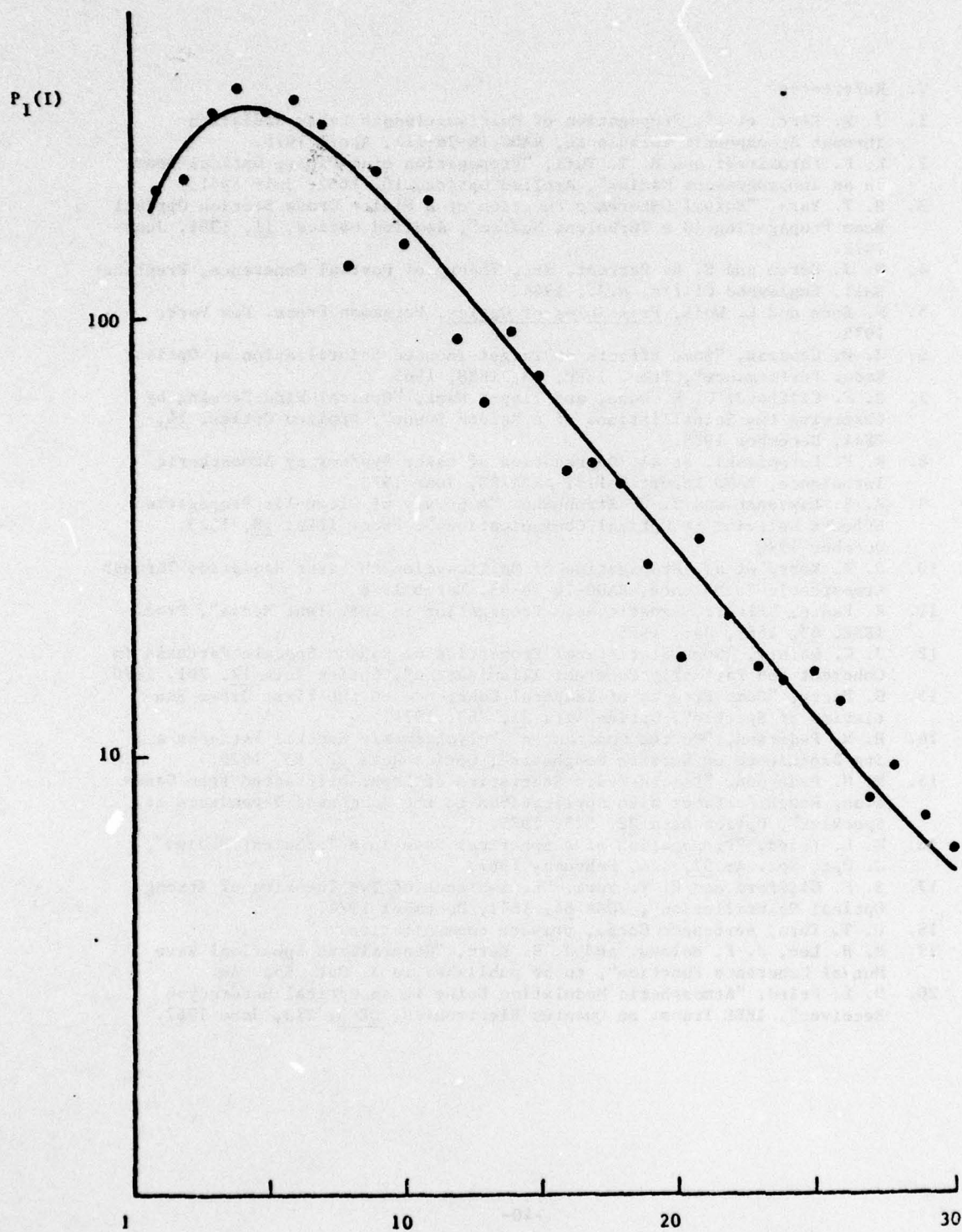


Figure 17. Measured Probability Distribution of Irradiance, Strong Turbulence
($L = 500\text{m}$, $\sigma_{I_N}^2 = 1.2$).

V. References

1. J. R. Kerr, et al, Propagation of Multiwavelength Laser Radiation Through Atmospheric Turbulence, RADC-TR-76-111, April 1976.
2. R. F. Lutomirski and H. T. Yura, "Propagation of a Finite Optical Beam in an Inhomogeneous Medium", *Applied Optics*, 10, 1652, July 1971.
3. H. T. Yura, "Mutual Coherence Function of a Finite Cross Section Optical Beam Propagating in a Turbulent Medium", *Applied Optics*, 11, 1399, June 1972.
4. M. J. Beran and G. B. Parrent, Jr., *Theory of Partial Coherence*, Prentice-Hall, Englewood Cliffs, N.J., 1964.
5. M. Born and E. Wolf, *Principles of Optics*, Pergamon Press, New York, 1975.
6. J. W. Goodman, "Some Effects of Target-Induced Scintillation on Optical Radar Performance", *Proc. IEEE*, 53, 1688, 1965.
7. S. F. Clifford, G. R. Ochs, and Ting-i Wang, "Optical Wind Sensing by Observing the Scintillations of a Random Scene", *Applied Optics*, 14, 2844, December 1975.
8. R. F. Lutomirski, et al, Degradation of Laser Systems by Atmospheric Turbulence, RAND Report R-1171-ARPA/RC, June 1973.
9. R. S. Lawrence and J. W. Strohbehn, "A Survey of Clean-Air Propagation Effects Relevant to Optical Communications", *Proc. IEEE*, 58, 1523, October 1970.
10. J. R. Kerr, et al, Propagation of Multiwavelength Laser Radiation Through Atmospheric Turbulence, RADC-TR-76-49, March 1976.
11. R. Fante, "Electromagnetic Beam Propagation in Turbulent Media", *Proc. IEEE*, 63, 1669, Dec. 1975.
12. J. C. Dainty, "Some Statistical Properties of Random Speckle Patterns in Coherent and Partially Coherent Illumination", *Optica Acta* 17, 761, 1970.
13. G. Parry, "Some Effects of Temporal Coherence on the First Order Statistics of Speckle", *Optica Acta* 21, 763, 1974.
14. H. M. Pederson, "On the Contrast of Polychromatic Speckle Patterns and its Dependence on Surface Roughness", *Optica Acta* 22, 15, 1975.
15. H. M. Pederson, "Second-Order Statistics of Light Diffracted from Gaussian, Rough Surfaces with Applications to the Roughness Dependence of Speckles", *Optica Acta* 22, 523, 1975.
16. D. L. Fried, "Propagation of a Spherical Wave in a Turbulent Medium", *J. Opt. Soc. Am.* 57, 175, February 1967.
17. S. F. Clifford and H. T. Yura, "Equivalence of Two Theories of Strong Optical Scintillation", *JOSA* 64, 1641, December 1974.
18. H. T. Yura, Aerospace Corp., private communication.
19. M. H. Lee, J. F. Holmes, and J. R. Kerr, "Generalized Spherical Wave Mutual Coherence Function", to be published in *J. Opt. Soc. Am.*
20. D. L. Fried, "Atmospheric Modulation Noise in an Optical Heterodyne Receiver", *IEEE Trans. on Quantum Electronics*, QE-3, 213, June 1967.

APPENDIX A. Generalized Point-Source Mutual Coherence Functions

The point-source mutual coherence functions are crucial to the utilization of the extended Huygens-Fresnel approach. The basic work on this problem was done by Yura; a complete generalization is being published by the present authors.¹⁹ In this appendix, we summarize the second-order functions of interest in this report.

We point out that, following the completion of the preceding report (Ref. 1), an integration error was discovered in Ref. 3, and the expressions given below incorporate appropriate corrections.

The general n^{th} -order MCF is

$$H(\bar{\rho}_1, \bar{\rho}_2, \dots, \bar{\rho}_{2n}; \bar{p}_1, \bar{p}_2, \dots, \bar{p}_{2n}) \\ = \langle \exp \{ \psi(\bar{\rho}_1, \bar{p}_1) + \psi^*(\bar{\rho}_2, \bar{p}_2) + \dots + \psi(\bar{\rho}_{2n-1}, \bar{p}_{2n-1}) + \psi^*(\bar{\rho}_{2n}, \bar{p}_{2n}) \} \rangle \quad (A1)$$

where $\psi = \chi + i\phi$.

Under certain assumptions discussed in Ref. 19, the primary result is

$$H_n(\bar{\rho}, \bar{p}) = \exp \left\{ -\frac{1}{2} \sum_{j=i+1}^{2n} \sum_{i=1}^{2n-1} (-1)^{1+j+1} D_{\psi ij} + 2 \sum_{j=1}^M \sum_{i=1}^{2n-2} C_{\chi 2j+i, i} \right\} \quad (A2)$$

where M is the number of j satisfying $2j+i=2n$ (for i even) and $2j+i=2n-1$ (for i odd). The wave structure function D_{ψ} and log amplitude covariance function C_{χ} comprise a generalization of those normally seen⁹ in the literature. They refer to complex phase or log amplitude quantities as a function of $(\bar{p}_j - \bar{p}_i)$ in the observation plane, for fields emanating from $\bar{\rho}_j$ and $\bar{\rho}_i$ in the "source" (target) plane.

The phase structure functions are given by

$$D_{\psi ij} = 1/\rho_0^{5/3} 16/3 \int_0^1 dt |(\bar{p}_i - \bar{p}_j)t + (1-t)(\bar{\rho}_i - \bar{\rho}_j)|^{5/3} \quad (A3)$$

19. M. H. Lee, J. F. Holmes, and J. R. Kerr, "Generalized Spherical Wave Mutual Coherence Function", to be published in J. Opt. Soc. Am.

where $\rho_0 = (0.545 C_n^2 L k^2)^{-3/5}$ is the turbulence-induced coherence scale and C_n^2 is the refractive index structure constant.

The log amplitude covariance function requires some discussion. In the first-order or weak-scattering case, the well-known result is

$$C_{\chi ij} = 0.132 \pi^2 k^2 L C_n^2 \int_0^1 dt \int_0^\infty du u^{-8/3} \sin^2 \left[\frac{Lu^2(1-t)t}{2k} \right] \times J_0 \left[u |(\bar{p}_i - \bar{p}_j)t + (1-t)(\bar{\rho}_i - \bar{\rho}_j)| \right] \quad (A4)$$

In the strong-scattering (saturation) case, the required two-point (p_i, p_j) function has not been derived. However, in many cases the one-point function suffices. A modification of the expression given in Ref. 17, such that the saturated point-source variance is unity, gives

$$C_{\chi}(\rho_i, \rho_j) = 0.17 \int_0^1 du \int_0^\infty dq e^{-q} J_0 \left\{ 5.69 u q^{-3/5} \frac{|\rho_i - \rho_j|}{\rho_0} \right\} \quad (A5)$$

This expression is the asymptotic form for arbitrarily strong scatterings; a more general expression is given in Ref. 17. The latter result should in principle be utilized in many cases, i.e., involving multiple scattering conditions. However, since it is a relatively recent development, it has not been widely used. It has been incorporated in the present report, where appropriate, including numerical evaluations.

We now consider special cases of interest:

(a) $n = 1$

$$H(\bar{\rho}_1, \bar{\rho}_2; \bar{p}_1, \bar{p}_2) = e^{-\frac{1}{2} D_{12}} \psi_{12} \quad (A6)$$

(b) $n = 2$

$$H(\bar{\rho}_1, \bar{\rho}_2, \bar{\rho}_3, \bar{\rho}_4; \bar{p}_1, \bar{p}_2, \bar{p}_3, \bar{p}_4) = e^{-\frac{1}{2}(D_{12} + D_{13} + D_{14} + D_{23} + D_{24} + D_{34}) + 2C_{X13} + 2C_{X24}} \quad (A7)$$

This is a generalization (double-arguments) of the earlier results of Ref. 20.

20. D. L. Fried, "Atmospheric Modulation Noise in an Optical Heterodyne Receiver", IEEE Trans. on Quantum Electronics, QE-3, 213, June 1967.

(c) $n = 2$

$$\bar{p}_1 = \bar{p}_2, \bar{p}_3 = \bar{p}_4$$

$$\begin{aligned} H(\bar{\rho}_1, \bar{\rho}_2, \bar{\rho}_3, \bar{\rho}_4; \bar{p}_1, \bar{p}_3) = & \\ \exp \left\{ \frac{-8}{3\rho_0^{5/3}} \left[\int_0^1 dt |(1-t)(\bar{\rho}_1 - \bar{\rho}_2)|^{5/3} - \int_0^1 dt |(\bar{p}_1 - \bar{p}_3)t + (1-t)(\bar{\rho}_1 - \bar{\rho}_3)|^{5/3} \right. \right. & \\ + \int_0^1 dt |(\bar{p}_1 - \bar{p}_3)t + (1-t)(\bar{\rho}_1 - \bar{\rho}_4)|^{5/3} & \\ + \int_0^1 dt |(\bar{p}_1 - \bar{p}_3)t + (1-t)(\bar{\rho}_2 - \bar{\rho}_3)|^{5/3} & \\ - \int_0^1 dt |(\bar{p}_1 - \bar{p}_3)t + (1-t)(\bar{\rho}_2 - \bar{\rho}_4)|^{5/3} & \\ + \left. \int_0^1 dt |(1-t)(\bar{\rho}_3 - \bar{\rho}_4)|^{5/3} \right] & \\ + 2C_\chi (\bar{p}_1 - \bar{p}_3, \bar{\rho}_1 - \bar{\rho}_3) + 2C_\chi (\bar{p}_1 - \bar{p}_3, \bar{\rho}_2 - \bar{\rho}_4) \Big\} & \end{aligned} \quad (A8)$$

(d) $n = 2$

$$\begin{aligned} \bar{p}_1 &= \bar{p}_2, \bar{p}_3 = \bar{p}_4 \\ \bar{\rho}_1 &= \bar{\rho}_2, \bar{\rho}_3 = \bar{\rho}_4 \end{aligned}$$

$$H(\bar{\rho}_1, \bar{\rho}_1, \bar{\rho}_3, \bar{\rho}_3; \bar{p}_1, \bar{p}_3) = 4C_\chi (\bar{p}_1 - \bar{p}_3, \bar{\rho}_1 - \bar{\rho}_3) \quad (A9)$$

(e) $n = 2$

$$\begin{aligned} \bar{p}_1 &= \bar{p}_2, \bar{p}_3 = \bar{p}_4 \\ \bar{\rho}_1 &= \bar{\rho}_4, \bar{\rho}_2 = \bar{\rho}_3 \end{aligned}$$

$$\begin{aligned}
H(\bar{\rho}_1, \bar{\rho}_3, \bar{\rho}_3, \bar{\rho}_1; \bar{p}_1, \bar{p}_3) = \exp \left\{ \frac{-8}{3\rho_0^{5/3}} \left[2 \int_0^1 dt |(1-t)(\bar{\rho}_1 - \bar{\rho}_3)|^{5/3} \right. \right. \\
- \int_0^1 dt |(\bar{p}_1 - \bar{p}_3)t + (1-t)(\bar{\rho}_1 - \bar{\rho}_3)|^{5/3} \\
+ 2 \int_0^1 dt |(\bar{p}_1 - \bar{p}_3)t|^{5/3} - \int_0^1 dt |(\bar{p}_1 - \bar{p}_3)t - (1-t)(\bar{\rho}_1 - \bar{\rho}_3)|^{5/3} \Big] \\
\left. + 2C_X(\bar{p}_1 - \bar{p}_3, \bar{\rho}_1 - \bar{\rho}_3) + 2C_X(\bar{p}_1 - \bar{p}_3, \bar{\rho}_3 - \bar{\rho}_1) \right\} \quad (A10)
\end{aligned}$$

The latter may be more simply written:

$$\begin{aligned}
H(\bar{\rho}, \bar{p}) = \exp \left\{ \frac{-1}{\rho_0^{5/3}} \left[2\rho^{5/3} + 2p^{5/3} - \frac{8}{3} \int_0^1 dt |\bar{p}t + (1-t)\bar{\rho}|^{5/3} \right. \right. \\
- \frac{8}{3} \int_0^1 dt |\bar{p}t - (1-t)\bar{\rho}|^{5/3} \Big] + 2C_X(\bar{p}, \bar{\rho}) + 2C_X(\bar{p}, -\bar{\rho}) \Big\} \quad (A11)
\end{aligned}$$

A special case of (A11) is

$$(f) \quad \bar{p} = 0$$

$$H(\bar{\rho}) = \exp \{4C_X(\bar{\rho})\} \quad (A12)$$

APPENDIX B. Time-Delayed Point-Source Mutual Coherence Functions

The MCF's of Appendix A are extended to the time-delayed case by invoking the Taylor hypothesis.⁹ The general expression (A2) for H applies, with $D_{\psi ij}$ and $C_{\chi ij}$ of Equations (A3, A4) modified as follows:

$$D_{\psi ij}(\bar{\rho}, \bar{p}, \tau) = \frac{1}{\rho_0^{5/3}} \frac{8}{3} \int_0^1 dt |(\bar{p}_i - \bar{p}_j)t - \bar{v}\tau_{ij} + (1-t)(\bar{\rho}_i - \bar{\rho}_j)|^{5/3} \quad (B1)$$

$$C_{\chi ij}(\bar{\rho}, \bar{p}, \tau) = 0.132 \pi^2 k^2 L C_n^2 \int_0^1 dt \int_0^\infty du u^{-8/3} \sin^2 \left[\frac{L u^2 (1-t) t}{2k} \right] \\ \times J_0 \left[u |(\bar{p}_1 - \bar{p}_j) t - \bar{v} \tau_{ij} + (1-t)(\bar{\rho}_1 - \bar{\rho}_j)| \right] \quad (B2)$$

where $\bar{v}(t)$ is the transverse wind velocity along the path, and τ_{ij} is the desired time-difference associated with (\bar{p}_1, \bar{p}_j) . We again let $\bar{p}_1 = \bar{p}_2, \bar{p}_3 = \bar{p}_4$; and $\tau_{ij} = \tau_{13} \equiv \tau$. The special cases of interest are

$$(a) \quad n = 1$$

$$\bar{p}_1 = \bar{p}_2$$

$$\bar{\rho}_1 - \bar{\rho}_2 \equiv r$$

$$H(\bar{r}, \tau) = e^{-\frac{1}{2} D_\psi(\bar{r}, 0, \tau)} \quad (B3)$$

$$(b) \quad n = 2$$

$$\bar{p}_1 = \bar{p}_2, \bar{p}_3 = \bar{p}_4$$

$$\bar{\rho}_1 = \bar{\rho}_2, \bar{\rho}_3 = \bar{\rho}_4$$

$$H(\bar{\rho}, \bar{p}, \tau) = \exp \{ 4 C_\chi(\bar{p}, \bar{\rho}, \tau) \} \quad (B4)$$

$$(c) \quad n = 2$$

$$\bar{p}_1 = \bar{p}_2, \bar{p}_3 = \bar{p}_4$$

$$\bar{\rho}_1 = \bar{\rho}_4, \bar{\rho}_2 = \bar{\rho}_3$$

$$H(\bar{\rho}, \bar{p}, \tau) = \exp \left\{ \frac{-8}{3 \rho_0^{5/3}} \left[2 \int_0^1 dt |(1-t)\bar{\rho}|^{5/3} \right. \right. \\ \left. \left. + 2 \int_0^1 dt |\bar{p}t - \bar{v}\tau|^{5/3} - \int_0^1 dt |\bar{p}t - \bar{v}\tau + (1-t)\bar{\rho}|^{5/3} \right] \right\}$$

$$\begin{aligned}
& - \int_0^1 dt \left| \bar{p}t - \bar{v}\tau - (1-t)\bar{\rho} \right|^{5/3} \Big] \\
& + 2C_\chi(\bar{p}, \bar{\rho}, \tau) + 2C_\chi(\bar{p}, -\bar{\rho}, \tau) \Big\}
\end{aligned}
\tag{B5}$$

METRIC SYSTEM

BASE UNITS:

Quantity	Unit	SI Symbol	Formula
length	metre	m	...
mass	kilogram	kg	...
time	second	s	...
electric current	ampere	A	...
thermodynamic temperature	kelvin	K	...
amount of substance	mole	mol	...
luminous intensity	candela	cd	...

SUPPLEMENTARY UNITS:

plane angle	radian	rad	...
solid angle	steradian	sr	...

DERIVED UNITS:

Acceleration	metre per second squared	...	m/s ²
activity (of a radioactive source)	disintegration per second	...	(disintegration)/s
angular acceleration	radian per second squared	...	rad/s ²
angular velocity	radian per second	...	rad/s
area	square metre	...	m ²
density	kilogram per cubic metre	...	kg/m ³
electric capacitance	farad	F	A·s/V
electrical conductance	siemens	S	A/V
electric field strength	volt per metre	...	V/m
electric inductance	henry	H	V·s/A
electric potential difference	volt	V	W/A
electric resistance	ohm	...	V/A
electromotive force	volt	V	W/A
energy	joule	J	N·m
entropy	joule per kelvin	...	J/K
force	newton	N	kg·m/s ²
frequency	hertz	Hz	(cycle)/s
illuminance	lux	lx	lm/m ²
luminance	candela per square metre	...	cd/m ²
luminous flux	lumen	lm	cd·sr
magnetic field strength	ampere per metre	...	A/m
magnetic flux	weber	Wb	V·s
magnetic flux density	tesla	T	Wb/m ²
magnetomotive force	ampere	A	...
power	watt	W	J/s
pressure	pascal	Pa	N/m ²
quantity of electricity	coulomb	C	A·s
quantity of heat	joule	J	N·m
radiant intensity	watt per steradian	...	W/sr
specific heat	joule per kilogram-kelvin	...	J/kg·K
stress	pascal	Pa	N/m ²
thermal conductivity	watt per metre-kelvin	...	W/m·K
velocity	metre per second	...	m/s
viscosity, dynamic	pascal-second	...	Pa·s
viscosity, kinematic	square metre per second	...	m ² /s
voltage	volt	V	W/A
volume	cubic metre	...	m ³
wavenumber	reciprocal metre	...	(wave)/m
work	joule	J	N·m

SI PREFIXES:

Multiplication Factors	Prefix	SI Symbol
1 000 000 000 000 = 10 ¹²	tera	T
1 000 000 000 = 10 ⁹	giga	G
1 000 000 = 10 ⁶	mega	M
1 000 = 10 ³	kilo	k
100 = 10 ²	hecto*	h
10 = 10 ¹	deka*	da
0.1 = 10 ⁻¹	deci*	d
0.01 = 10 ⁻²	centi*	c
0.001 = 10 ⁻³	milli	m
0.000 001 = 10 ⁻⁶	micro	μ
0.000 000 001 = 10 ⁻⁹	nano	n
0.000 000 000 001 = 10 ⁻¹²	pico	p
0.000 000 000 000 001 = 10 ⁻¹⁵	femto	f
0.000 000 000 000 000 001 = 10 ⁻¹⁸	atto	a

* To be avoided where possible.

*MISSION
of
Rome Air Development Center*

RADC plans and conducts research, exploratory and advanced development programs in command, control, and communications (C³) activities, and in the C³ areas of information sciences and intelligence. The principal technical mission areas are communications, electromagnetic guidance and control, surveillance of ground and aerospace objects, intelligence data collection and handling, information system technology, ionospheric propagation, solid state sciences, microwave physics and electronic reliability, maintainability and compatibility.

